

Global Biogeochemical Cycles®

RESEARCH ARTICLE

10.1029/2021GB007068

Key Points:

- Soil carbon release due to permafrost degradation overwhelms net primary production on the Qinghai-Tibetan Plateau
- Deep soil nitrogen addition from thawing permafrost has a limited benefit to plant carbon uptake
- Permafrost degradation has more pronounced influences on carbon cycling of alpine meadows than alpine steppes

Supporting Information:

Supporting Information may be found in the online version of this article.

Correspondence to:

D. Zhao,
zhaods@igsnr.ac.cn

Citation:





Liu, L., Zhuang, Q., Zhao, D., Zheng, D., Kou, D., & Yang, Y. (2022). Permafrost degradation diminishes terrestrial ecosystem carbon sequestration capacity on the Qinghai-Tibetan plateau. *Global Biogeochemical Cycles*, 36, e2021GB007068. <https://doi.org/10.1029/2021GB007068>

Received 8 MAY 2021

Accepted 28 JAN 2022

© 2022. American Geophysical Union.
All Rights Reserved.

Permafrost Degradation Diminishes Terrestrial Ecosystem Carbon Sequestration Capacity on the Qinghai-Tibetan Plateau

Lei Liu^{1,2,3} , Qianlai Zhuang³ , Dongsheng Zhao¹ , Du Zheng^{1,2}, Dan Kou^{3,4} , and Yuanhe Yang^{2,5} 

¹Key Laboratory of Land Surface Pattern and Simulation, Institute of Geographical Sciences and Natural Resources Research, Chinese Academy of Sciences, Beijing, China, ²University of Chinese Academy of Sciences, Beijing, China, ³Department of Earth, Atmospheric, and Planetary Sciences, Purdue University, West Lafayette, IN, USA, ⁴Biogeochemistry Research Group, Department of Environmental and Biological Sciences, University of Eastern Finland, Kuopio, Finland, ⁵State Key Laboratory of Vegetation and Environmental Change, Institute of Botany, Chinese Academy of Sciences, Beijing, China

Abstract Effects of permafrost degradation on carbon (C) and nitrogen (N) cycling on the Qinghai-Tibetan Plateau (QTP) have rarely been analyzed. This study used a revised process-based biogeochemical model to quantify the effects in the region during the 21st century. We found that permafrost degradation would expose 0.61 ± 0.26 (mean \pm SD) and 1.50 ± 0.15 Pg C of soil organic carbon under the representative concentration pathway (RCP) 4.5 and the RCP 8.5, respectively. Among them, more than 20% will be decomposed, enhancing heterotrophic respiration by 8.62 ± 4.51 (RCP 4.5) and 33.66 ± 14.03 (RCP 8.5) Tg C/yr in 2099. Deep soil N supply due to thawed permafrost is not accessible to plants, only stimulating net primary production by 7.15 ± 4.83 (RCP 4.5) and 24.27 ± 9.19 (RCP 8.5) Tg C/yr in 2099. As a result, the single effect of permafrost degradation would cumulatively weaken the regional C sink by 209.44 ± 137.49 (RCP 4.5) and 371.06 ± 151.70 (RCP 8.5) Tg C during 2020–2099. However, when factors of climate change, CO₂ increasing and permafrost degradation are all considered, the permafrost region on the QTP would be a stronger C sink in the 21st century. Permafrost degradation has a greater influence on C balance of alpine meadows than alpine steppes on the QTP. The shallower active layer, higher soil C and N stocks, and wetter environment in alpine meadows are responsible for its stronger response to permafrost degradation. This study highlights that permafrost degradation could continue to release large amounts of C to the atmosphere irrespective of potentially more nitrogen available from deep soils.

1. Introduction

Permafrost degradation due to climate warming makes large amounts of frozen soil organic matter (SOM) available for decomposition, leading to positive feedback to the climate system by releasing greenhouse gases into the atmosphere (Koven et al., 2011; Koven, Schuur et al., 2015; Schaefer et al., 2014; Schuur et al., 2015). Enhanced decomposition in permafrost regions also increases nutrient availability, however (Keuper et al., 2012; Salmon et al., 2016, 2018), stimulating plant production. Together with the effects of increasing air temperature, expanding growing season, shifting plant community composition, and rising atmospheric CO₂ concentration, increased nutrient availability due to permafrost thaw could also result in negative feedback to climate warming (Finger et al., 2016; Liang et al., 2018; X. Peng et al., 2020; Zhuang et al., 2010). Considerable uncertainty of these positive and negative feedbacks limits our ability to model C balance of the permafrost region (Abbott et al., 2016).

Models that coupled the impact of permafrost degradation into land surface have projected that the northern high latitudes would shift from a net C sink (Qian et al., 2010) to a net source to the atmosphere (Burke et al., 2013; Koven et al., 2011; MacDougall and Knutti, 2016; Schaefer et al., 2014; Schaphoff et al., 2013). However, large uncertainties still exist in the magnitude of the estimated changes in soil, vegetation, and ecosystem C stocks (McGuire et al., 2016). Model structural differences, particularly in the soil carbon decomposition processes, have been attributed to be the largest uncertainty in quantifying permafrost carbon-climate feedbacks (Burke et al., 2017).

A critical model structural feature to represent the permafrost carbon-climate feedback is to consider soil C exposure with thaw depth (McGuire et al., 2018). In permafrost regions, part of soil organic carbon (SOC) is protected from decomposition by frozen soil but may become more susceptible to decomposition with warm-

ing-induced degradation of permafrost. To better account for the influence of permafrost dynamics on terrestrial carbon balance, soil C exposure due to thawing permafrost should be incorporated into land surface models. Hayes et al. (2014) assessed the net effect of active layer dynamics on permafrost carbon feedback during 1970–2006 over the circumpolar permafrost region. They found that permafrost degradation exposed 11.6 Pg C of SOM, and the decomposition of these newly exposed SOM resulted in 4.03 Pg C emission; however, only 0.3 Pg C was compensated by net primary production (NPP). Using a carbon-nitrogen model that includes permafrost processes and depth-dependent changes in SOM, Koven, Lawrence, and Riley (2015) found similar results and projected that permafrost carbon-climate feedback is sensitive to deep soil carbon decomposability, and the impact of deep soil nitrogen mineralization on C budget is small. However, projections of five biogeochemical models that represent soil C explicitly with depth showed that the northern permafrost region would likely act as a net C sink before 2100 due to stronger vegetation C uptake (McGuire et al., 2018). The different results found by McGuire et al. (2018) may be due to the lower (less than three m) active layer thickness (ALT) considered in their study. The decomposition of large quantities of deep carbon deposits (Schuur et al., 2015) may reverse this estimation.

The Qinghai-Tibetan Plateau (QTP) is characterized by a deep ALT (2.34 ± 0.70 m), and about 15% of the QTP permafrost region has ALT greater than 3 m (T. Wang et al., 2020). SOC storage on the QTP is estimated at 50.43 Pg, of which 35.10 Pg stores below 3 m soils and 37.21 Pg frozen in permafrost currently (T. Wang et al., 2020). Based on the vertical distribution of SOC and the change of ALT, T. Wang et al. (2020) estimated that permafrost thaw on the QTP would expose 1.86 ± 0.49 to 3.80 ± 0.76 Pg frozen C to decomposition, which could potentially turn the region from a net C sink to a net source. The lack of the simulation of SOM decomposition, and the use of net biome production (NBP) from CMIP5 models (which did not consider permafrost carbon [Jones et al., 2016] and hence the stimulation of vegetation production due to N supply from thawed permafrost), may bias the estimation of net C budget in the study of T. Wang et al. (2020). Through repeated soil carbon measurements on the QTP, Ding et al. (2017) suggested that the upper active layer of the QTP permafrost currently represents a substantial regional soil C sink, probably owing to enhanced vegetation growth. However, this study only examined SOC stocks in uppermost 30 cm. Carbon changes associated with deeper and older permafrost remain largely unknown (Mu et al., 2020). Inadequate studies that focus on representing soil C explicitly with depth, particularly representing soil C in deep soils, and simultaneously consider the feedback of vegetation to permafrost thaw impedes our understanding of permafrost carbon-climate feedbacks on the QTP.

Apart from deep ALT, the environment of the permafrost regions on the QTP is also different from the pan-Arctic in water conditions. Specifically, annual precipitation decreases from southeastern to northwestern on the QTP. As a result, the eastern QTP receives more precipitation and is dominated by alpine meadow ecosystem, while the widespread inner and western parts are controlled by alpine arid climate and dominated by alpine steppe ecosystems. Many studies have found that the alpine steppe and alpine meadow ecosystems respond differently to climate change (Hao et al., 2021; S. Li et al., 2019; Liu et al., 2020; F. Peng et al., 2020). For example, a warming experiment revealed that warming increased plant productivity in alpine meadows but decreased productivity in alpine steppes (Ganjurjav et al., 2016). Temperature sensitivity of ecosystem respiration (Q10) in alpine meadows (3.4) can be twice the number in alpine steppes (1.7; L. Wang et al., 2018). The distinct environment and the different responses to climate change of these two ecosystems could result in different permafrost C feedbacks. However, currently the effects of active layer deepening on C balance of these two ecosystems are still not certain.

In this study, a process-based biogeochemical model was revised by coupling thaw depth with soil C exposure to analyze the following issues: (a) the quantity of frozen SOC in deep soils on the QTP that will be exposed to decomposition due to permafrost thaw in the 21st century, and the quantity of C that will be released into the atmosphere; (b) the stimulation of deep permafrost thaw on vegetation productivity due to extra N supply, and the net effect of permafrost thaw on ecosystem C balance (enhanced heterotrophic respiration (RH) versus stimulated net primary production (NPP)); and (c) the different responses of C balance of the distinct alpine meadow and alpine steppe ecosystems to permafrost thaw.

2. Methods and Data

2.1. The Terrestrial Ecosystem Model

The Terrestrial Ecosystem Model (TEM) is a process-based, global-scale biogeochemical model, using spatially explicit soil, vegetation, and elevation data, and climate forcing of radiation, precipitation, and air temperature to

simulate ecosystem C and N cycling (McGuire et al., 1992; Zhuang et al., 2002). A brief introduction of TEM can be found in Text S1 in Supporting Information S1. A soil thermal model (Text S2 in Supporting Information S1) has been coupled into TEM to represent vertical soil thermal profile in permafrost- and nonpermafrost-dominated ecosystems and given TEM the ability to describe freeze-thaw cycles in cold regions (Z. Jin et al., 2015; Zhuang et al., 2001, 2010). The effects of freeze-thaw dynamics on gross primary production (GPP) have also been considered in TEM (Zhuang et al., 2011). TEM has been extensively used to evaluate C dynamics in northern high latitudes and Tibet plateau (e.g., Hayes et al., 2014; Z. Jin et al., 2013, 2015; Kicklighter et al., 2019; McGuire et al., 2018).

In previous versions of TEM, soil organic carbon (SOC) in the entire root zone is assumed to be available for decomposition, and thus take part in heterotrophic respiration. However, since active layer thicknesses (ALT) in permafrost regions are often shallower than root depth defined in TEM (Hayes et al., 2011, 2014), part of SOC in root zone is frozen in soil and protected from microbial decomposition. Therefore, SOC considered in heterotrophic respiration should be smaller than the entire SOC stock in root zone. TEM6 (Hayes et al., 2011, 2014) has considered the amount of SOC available for decomposition and treated it as a proportion of the entire root zone SOC, depending upon the ratio of ALT to rooting depth. By calculating ALT variation over time through the soil thermal module in TEM, this approach has been used to estimate the potential influence of permafrost thaw on the availability of soil organic matter to decomposition (Hayes et al., 2014; Kicklighter et al., 2019). However, this approach did not consider SOC below the rooting zone and assumed that they do not contribute to C flux. When warming continues in the future, and ALT deepens below rooting depth, this approach may underestimate the influence of permafrost degradation on the availability of carbon to decomposition (Hayes et al., 2011).

On the QTP, ALT (2.34 m; T. Wang et al., 2020) is usually much deeper than rooting depth (over 90% of plant roots are distributed within the top 30 cm soil layer; Y. Yang et al., 2009). Future permafrost degradation would probably happen far below rooting zone. Therefore, we modified the approach by adjusting SOC according to the ratio of ALT of current time step to previous time step, rather than the ratio of ALT to rooting zone depth:

$$\text{SOC}_i = \text{SOC}_{i-1} * \left(1 + \frac{\text{prop}_i - \text{prop}_{i-1}}{\text{prop}_{i-1}} \right) \quad (1)$$

$$\text{prop}_i = \frac{a * \text{ALT}_i}{b + \text{ALT}_i} \quad (2)$$

where i and $i-1$ denote the current and previous year, respectively; ALT_i is the maximum ALT of the current year; prop_i denotes the proportion of SOC in the active layer of the current year to the total SOC in the entire soil profile. The hyperbolic function of prop_i describes the vertical distribution of SOC in soil profile, with a high density of SOC in shallow soil layers but decreases toward deep soil, as documented by Hayes et al. (2014). a and b are parameters controlling the shape of the curve that how SOC density changes with soil depth. We estimated parameter b for alpine meadow, alpine steppe, and alpine desert ecosystems using observation data (Figure S1 in Supporting Information S1). For the remaining ecosystems, we set parameters b according to Kicklighter et al. (2019). Parameter values of b for main ecosystems on the QTP are listed in Table S1 in Supporting Information S1. Parameter a will be divided when putting Equation 2 into Equation 1. According to a recent study (T. Wang et al., 2020), SOC density on the QTP does not always decrease with soil depth. Below three m, SOC density fluctuates around the value of three m' and does not show a clear increasing or decreasing trend until 25 m. Therefore, we estimated SOC according to Formulas 1 and 2 for top three m of soil profile and assumed that SOC density is uniform below three m.

Using this method, SOC within thawed permafrost was factored into total available SOC pools for soil decomposition. Although we considered the fact that SOC density decreases with soil depth, the vertical variations in SOC turnover time are still missing in this study, which may overestimate SOC decomposition rate to some extent (Shu et al., 2020). It should also be noted that SOC hereinafter in this study refers to total available SOC pools in active layer.

Permafrost degradation influences not only the amount of SOC, but also soil organic N (SON), available inorganic N, and soil water content. These variables were also adjusted according to the variation of ALT, using the same method as that for SOC. However, although permafrost degradation can increase available N pools, if ALT

deepens far below rooting depth, we assume that the additional N cannot be accessed by vegetation. Therefore, only N in rooting zone was used for vegetation N uptake calculation when ALT is greater than rooting zone depth.

Two freezing fronts are modeled in TEM (as shown in Text S2 in Supporting Information S1), including freezing down due to cold air temperature and freezing up due to permafrost underneath the soils (Zhuang et al., 2001). ALT in permafrost regions is calculated as the total depth of unfrozen soil layers above the two freezing fronts. TEM does not explicitly “define” permafrost occurrence in a grid cell, but infer its depth based on the 0°C isotherm in the soil thermal profile. The study area was defined as the current permafrost domain on the QTP, which was derived from the permafrost map of China (T. Wang, 2019). Soil temperature and active layer depth were estimated with the model using the permafrost distribution data. C and N dynamics were then modeled driven by simulated soil thermal dynamics in the region.

2.2. Model Calibration and Validation

TEM has been calibrated for terrestrial ecosystems on the QTP by Zhuang et al. (2010) and Z. Jin et al. (2013, 2015). Localized parameters for six major vegetation types on the QTP, including alpine steppe, alpine meadow, alpine cushion, alpine desert, alpine shrubland, and forest ecosystems, have also been developed by these studies. In this study, key parameters related to ecosystem C and N cycling (Zhu & Zhuang, 2014; such as the maximum rate of photosynthesis, heterotrophic respiration, and plant N uptake and respiration rate) were recalibrated for three major ecosystems (i.e., alpine shrubland, alpine meadow, and alpine steppe), which occupy 82.6% of the permafrost regions on the plateau according to the 1:1,000,000 vegetation map of China (Figure 1a; Editorial Committee of Vegetation Map of China, Chinese Academy of Sciences, 2001). These parameters were optimized by minimizing the differences between observations and simulations through altering parameters and iterating model simulations. Other parameters, such as the ones regulating heat transfer in soil profile and hydrological processes, and the ones controlling model running, were set as previous studies (Zhuang et al., 2010; Z. Jin et al., 2013, 2015). Calibrated parameters and their optimal values are listed in Table S2 in Supporting Information S1. Site information of these three ecosystems is provided in Table S3 in Supporting Information S1. During the processes of model calibration, observational climate data at each site were used for model spin-up and simulation. TEM was first run up to 3,000 times to reach equilibrium with the first year's climate data, then spin up for 200 years before the transient simulation.

The model was validated with 289 observations (Figure 1a) of soil C and N pools (data derived from Ding et al., 2016, Kou et al., 2019, and T. Wang et al., 2020) on the plateau. These observation sites spread over alpine desert, alpine steppe, alpine meadow, and alpine cushion ecosystems on the QTP. Other 43 observations of ALT (Figure 1a), derived from the Circumpolar Active Layer Monitoring Network (CALM, <https://www2.gwu.edu/~calm/data/north.htm>), Qin et al. (2017), and Q. Wu et al. (2012), were used to validate simulated ALT. ALT observations were collected between 2006 and 2012. The simulated ALT during this period was averaged first before validation. During the validation, we first located the observations into model grids and then compared the observations with model results in corresponding model grids.

2.3. Simulation Protocol

Spatial resolution for regional simulation was 0.1° latitude by 0.1° longitude. All input data were gridded to the same spatial resolution.

To determine the direct effects of ALT deepening on ecosystem C dynamics, we carried out two simulations: the referenced simulation (S_R) and the transient simulation (S_T). The two simulations share the same model inputs but differ in model structure. They are identical until 2020. After that, ALT changes with climate in S_T but remains constant in S_R . Therefore, C and N pools do not change with ALT in S_R after 2020 but are influenced by ALT in S_T . Through comparing the results of these two simulations, the direct effects of ALT changes on ecosystem C dynamics can be estimated. The differences between the results of S_T and S_R (i.e., $S_T - S_R$) are referred to as Δ hereinafter.

For each grid cell, historical data from 1861 to 1900 were used to spin up the model repeatedly for 200 years until dynamic equilibriums for C and N pools were achieved. The state variables of the dynamic equilibrium were then used as the initial value for a historical simulation from 1901 to 2020. From the same model state at 2020, S_T differed from S_R in the remaining simulations from 2021 to 2099.

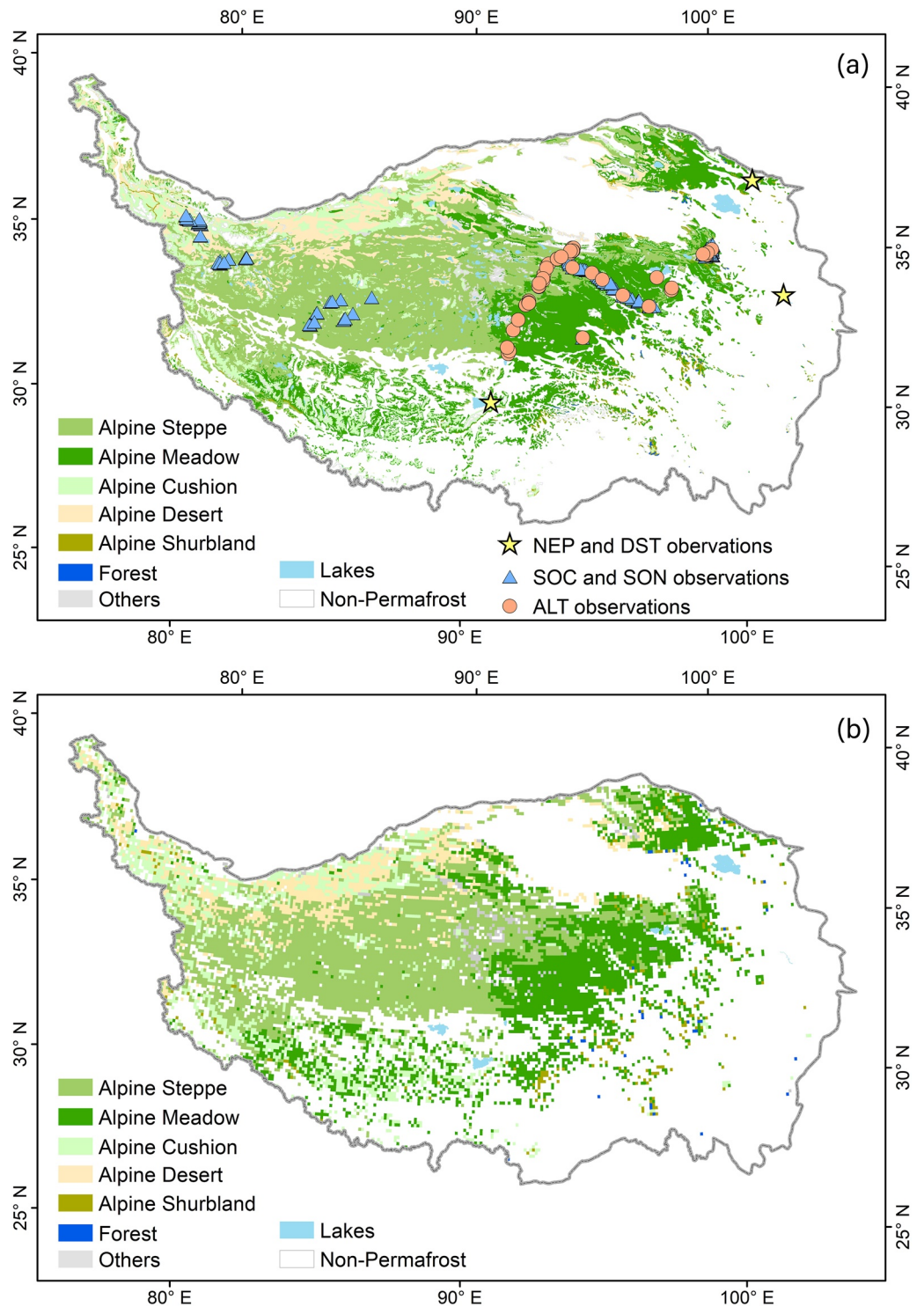


Figure 1. Vegetation distribution in the permafrost regions of the QTP. The vegetation distribution map (a) was derived from a 1:1,000,000 vegetation map of China (Editorial Committee of Vegetation Map of China, Chinese Academy of Sciences, 2001) provided by the Resources and Environment Science Data Center, Chinese Academy of Sciences. The permafrost map (all the colored patches exclude lakes) was obtained from frozen ground map of China (T. Wang, 2019). Yellow stars, pink dots, and blue triangles are locations of net ecosystem production (NEP)/soil temperature (DST), active layer thickness (ALT), and soil organic C and N stocks (SOC/SON) observations, used for model validation of NEP/DST, ALT and SOC/SON, respectively. (b) The vegetation map (0.1° latitude by 0.1° longitude) of the permafrost region on the QTP prescribed in TEM model.

2.4. Data

TEM was driven by spatially referenced information on climate, soils, vegetation, and elevation for spatial extrapolation.

Climate data, including air temperature ($^{\circ}\text{C}$), precipitation (mm), and incident shortwave solar radiation (W/m^2) from 1861 to 2099, were derived from four global circulation models (GCMs: IPSL-CM5A-LR, GFDL-ESM2M, MIROC5, and HadGEM2-ES) in the second simulation round of the Inter-Sectoral Impact Model Intercomparison Project (ISI-MIP 2b). Known issues of previous rounds of ISI-MIP have been solved for the ISI-MIP 2b through a series of adjustments, and atmospheric data provided by the ISI-MIP 2b have also been bias-adjusted to a new reference data set of EWEMBI (Frieler et al., 2017). Regional simulation of this century was conducted under two climate scenarios of the Representative Concentration Pathway 4.5 (RCP 4.5) and RCP 8.5, which correspond to radiative forcing levels of 4.5 and 8.5 W/m^2 by 2100, respectively (Moss et al., 2010).

Soil texture data over the QTP were based on the RegridDED Harmonized World Soil Database v 1.2 (Wieder, 2014). Vegetation (Figure 1a) and elevation data were derived from the 1:1,000,000 vegetation map of China (Editorial Committee of Vegetation Map of China, Chinese Academy of Sciences, 2001) and the Shuttle Radar Topography Mission (SRTM; Farr et al., 2007), respectively. The vegetation map of the permafrost region on the QTP prescribed in TEM model is shown in Figure 1b.

The spatial resolutions of soil texture and elevation data are 0.05° and 90 m, respectively. Compared with these land surface datasets, the climate data are much coarser, at the spatial resolution of 0.5° . On the QTP, topography, vegetation and soil may change greatly within 0.5° spatial resolution. To consider the effects of heterogeneities of these data, we resampled climate data into a spatial resolution of 0.1° . During resampling, we make every 25 grids of the resampled climate data share the same value as the grid of the same location of the original climate data. We did not adjust climate data according to elevation, which may introduce uncertainty. TEM is run on a monthly time scale. We averaged the daily climate data to monthly before resampling.

3. Results

3.1. Model Validation

We validated TEM with monthly observation data of soil temperature and NEP for three dominant ecosystems on the QTP (Figure 1). TEM well reproduced the seasonal variation of soil temperature and NEP at all sites, with R^2 greater than 0.9 and 0.8 for soil temperature and NEP, respectively. Simulated SOC and SON at these three sites are close to observations (Table S3 in Supporting Information S1).

The comparison between the calculated and measured ALT (Figure 2g) shows that the simulated ALT is significantly correlated with observations, with R^2 greater than 0.8 and root mean square error (RMSE) for all the 43 observations being 0.35 cm. This comparison suggests that TEM performs well in simulating ALT on the QTP.

We also compared the simulated SOC and SON with 289 observations on the Plateau (Figures 2h and 2i and Figure S2 in Supporting Information S1). There are some discrepancies between modeled and observed SOC and SON, which may be due to the following reasons. First, the calculated SOC and SON in this study are C and N stocks in active layers, while the observations represent C and N stocks in top two m (top three m for 173 SON observations; Kou et al., 2019) of soil profile. According to Ding et al. (2016), Kou et al. (2019), and T. Wang et al. (2020), about half of the observation sites are distributed in the regions where ALT is estimated less than two m. As a result, the simulated SOC and SON in active layer are smaller than observations (Figure 2). Second, although the heterogeneities in topography, vegetation, and soils were considered by running the model on $0.1^{\circ} \times 0.1^{\circ}$ of spatial resolution, the great spatial heterogeneities in SOC (Mishra et al., 2021) and SON made it difficult to predict site-level observations precisely based on large grid simulations.

In general, the simulated SOC and SON are comparable to observations based on the means across vegetation types (Figure 2). For the entire permafrost regions on the QTP, the estimated SOC stock in active layers during 2006–2015 under the RCP 4.5 scenario is 13.75 ± 0.98 Pg C (mean \pm SD), which is comparable to the 13.22 Pg C estimated by T. Wang et al. (2020), but lower than the 19.0 ± 6.6 Pg C (in 0–2 m soils) estimated by Mu et al. (2020). SON stocks in alpine grassland active layers during 2013–2014 are estimated at 1.08 ± 0.07 kg N/m², which is below the range of 1.40–1.76 kg N/m² from observation data within 0–3 m soil depth (Kou

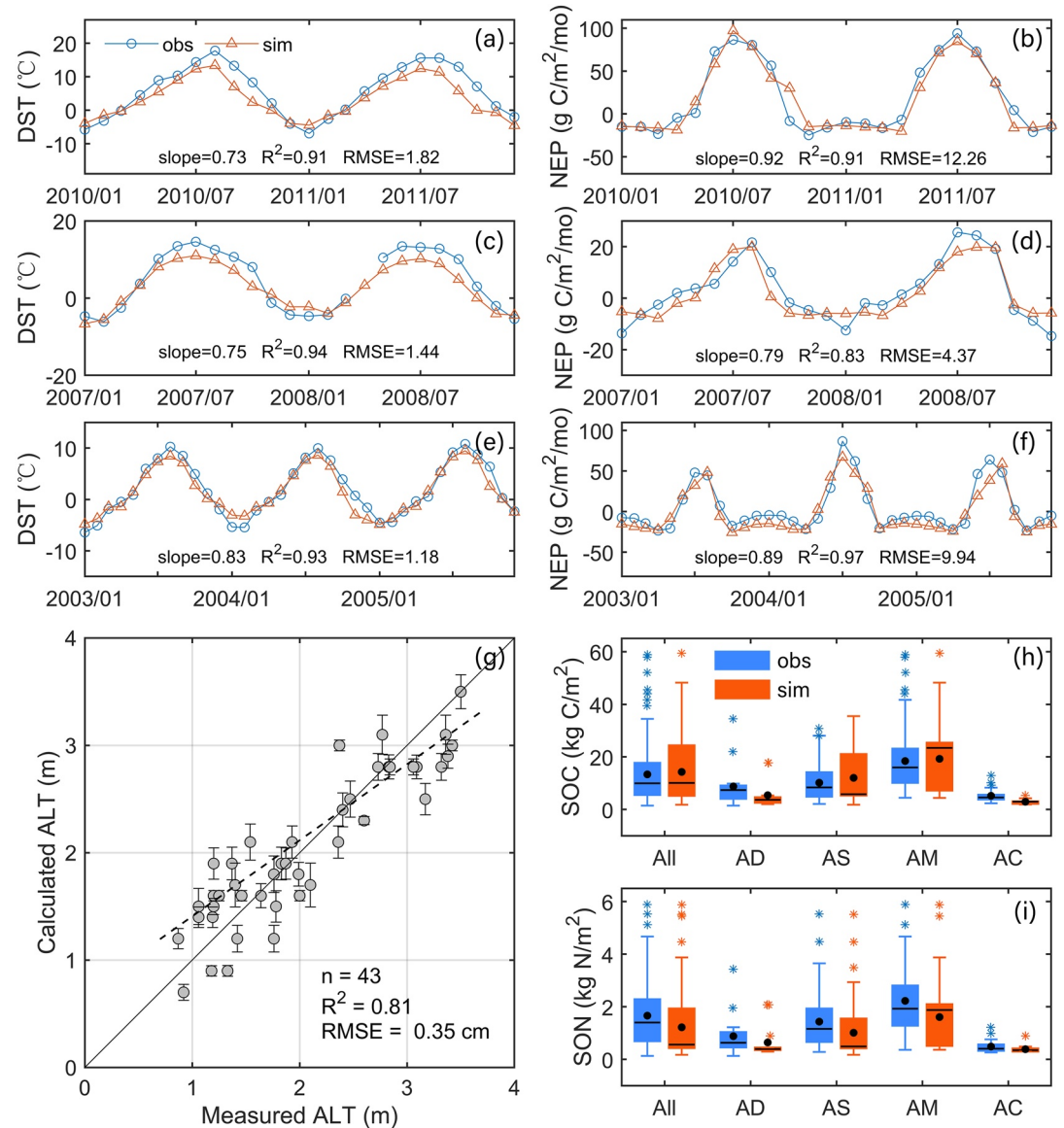


Figure 2. Comparison between simulation (sim) and observations (obs) for soil temperature (DST) and NEP at alpine meadow (a) and (b), alpine steppe (c) and (d), and alpine shrub (e) and (f) sites, respectively. RMSE denotes Root Mean Square Error. See Table S3 in Supporting Information S1 for detailed information of the observation sites. **g** is the comparison of measured and calculated active layer thickness (ALT) across the QTP. **h** and **i** represent the comparison of the simulated SOC and SON with 289 observations for alpine desert (AD), alpine steppe (AS), alpine meadow (AM), and alpine cushion (AC) on the Plateau. The number of observation sites for AD, AS, AM, and AC are 16, 134, 106, and 33, respectively. Site-by-site comparison of simulated SOC and SON with observations is shown in Figure S2 in Supporting Information S1.

et al., 2019). The estimation of SON in this study is within active layer (2.68 ± 0.09 m) other than 3 m depth in the study of Kou et al. (2019), which may result in the difference. The estimated NPP of the whole QTP is 235.68 ± 10.56 g C/m²/yr during 2002–2012, which is located in the middle of a MODIS normalized difference vegetation index (NDVI) based estimation of 219.8–242.5 g C/m²/yr (S. Wang et al., 2017).

3.2. Changes in Ecosystem C Balance and the Effects of ALT Deepening

Permafrost regions on the QTP are projected to be a stronger C sink during the remaining of the 21st century. NPP and RH both increase under the RCP 4.5 and RCP 8.5 (Figure S3 in Supporting Information S1, S_T). Under the RCP 8.5, the increase in NPP (127.47 ± 24.07 Tg C/yr) is much higher than RH (89.99 ± 23.50 Tg C/yr).

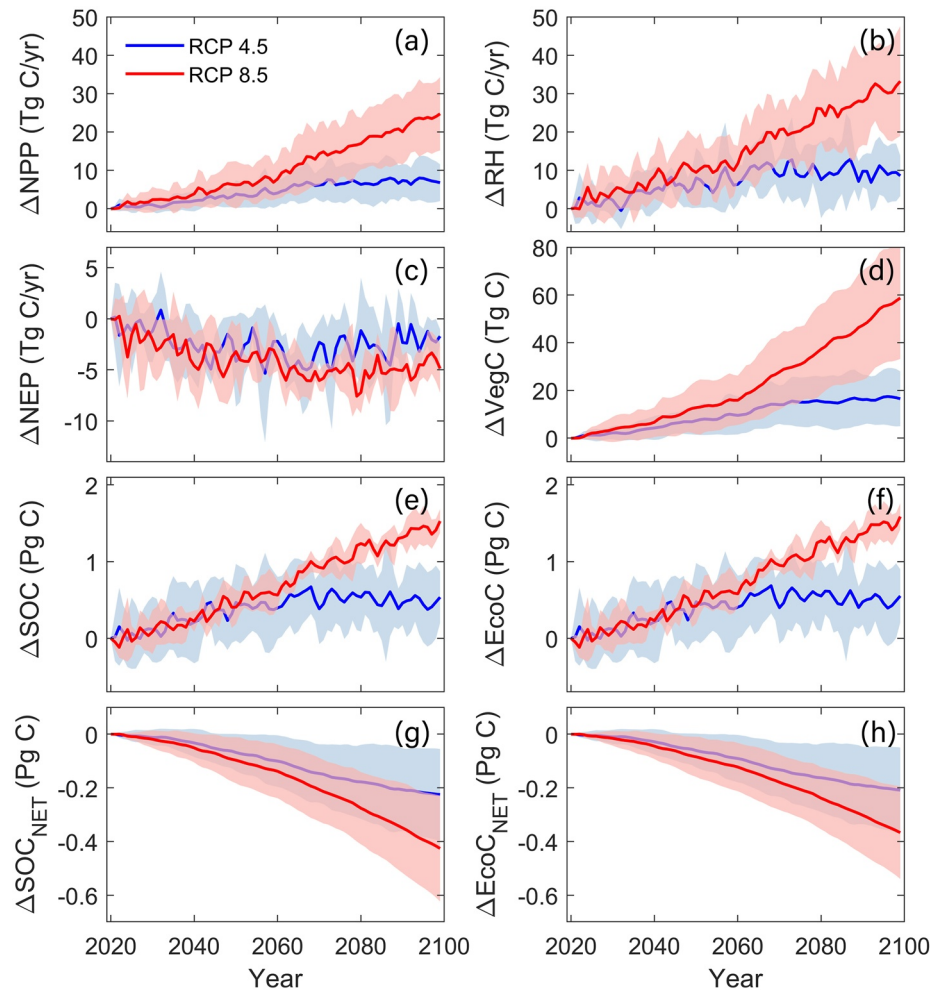


Figure 3. Effects of ALT deepening on ecosystem C balance of permafrost regions on the QTP under the RCP 4.5 and RCP 8.5 scenarios. Δ means the difference between the results of the transient simulation and the referenced simulation ($S_T - S_R$). Δ SOC is the change of SOC stock due to ALT deepening, including the additional C from thawing permafrost. Δ SOC_{NET} subtracts these additional C from Δ SOC to indicate net C change of entire soil layers. Δ EcoC and Δ EcoC_{NET} is the sum of Δ VegC (vegetation C) and corresponding SOC. Blue and red shade denote the standard deviation of all GCMs for the RCP 4.5 and RCP 8.5 simulations, respectively.

However, under the RCP 4.5, the increases in NPP and RH are comparable, which are 48.62 ± 10.47 Tg C/yr and 48.17 ± 12.65 Tg C/yr, respectively. As a result, NEP increases by 0.45 ± 2.41 (RCP 4.5) and 41.09 ± 6.28 (RCP 8.5) Tg C/yr during 2020–2099. Permafrost regions on the QTP would sequester more C under the RCP 8.5.

The effects of ALT deepening on C balance are represented by the difference between S_T and S_R . Figure 3 shows that ALT deepening has evident effects on C balance. We calculated the contribution of ALT deepening effects to C balance change by dividing the difference in S_T and S_R from overall C balance changes (Figure 4b). Under the RCP 4.5, ALT deepening can contribute 13%–23% of the C balance changes, and the contributions increase to 17%–35% under the RCP 8.5. The radical change in ALT (Figure 4a) under the RCP 8.5 results in a greater contribution. Under both RCPs, the deepening of ALT has more influence on SOC and RH than vegetation C and NPP (Figures 3 and 4b).

Although both NPP and RH increase more in S_T than S_R (Figure S3 in Supporting Information S1) under both RCPs, the increase in Δ RH (8.56 ± 5.28 [RCP 4.5] and 33.22 ± 14.30 [RCP 8.5] Tg C/yr) is greater than Δ NPP (6.76 ± 4.78 [RCP 4.5] and 24.73 ± 9.56 [RCP 8.5] Tg C/yr) due to ALT deepening (Figure 3), resulting in smaller NEP in S_T than S_R (Figure S3 in Supporting Information S1). Moreover, Figure 3e shows that ALT deepening increases SOC. However, Δ SOC also includes additional C from thawed permafrost (SOC_{pf}), which

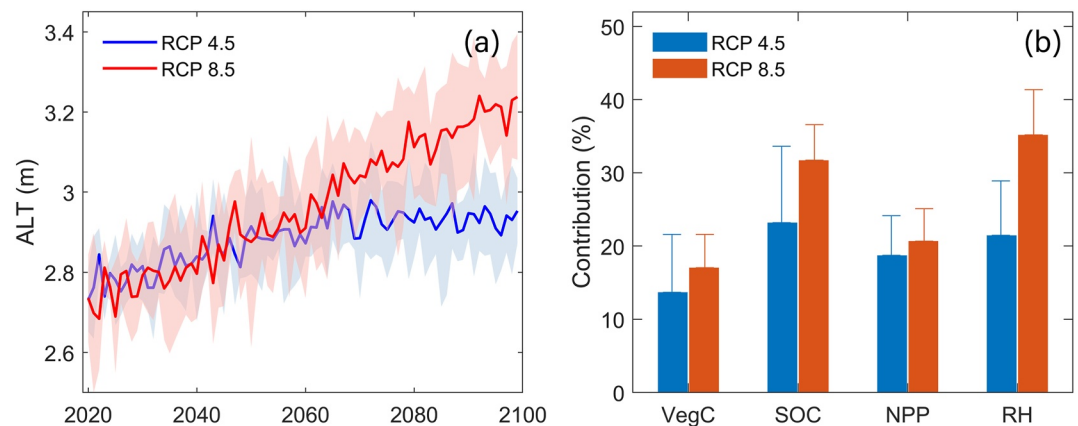


Figure 4. (a) Changes in mean ALT of the QTP under the RCP 4.5 and RCP 8.5 scenarios; (b) Contributions of ALT deepening effects to the overall C balance changes caused by climate change in permafrost regions of QTP during the 21st century. The shade in (a) and error bars in (b) denotes the standard deviation among all GCMs.

just transforms from frozen SOC in permafrost into available SOC for decomposition in active layer, but not new SOC added to the entire soil profile. When subtracting SOC_{PF} (which can be calculated from soil C balance) from ΔSOC , the remaining is the net change of total SOC in active layer and permafrost due to ALT deepening (ΔSOC_{NET}). Figure 3g shows that the single effect of ALT deepening would decrease total SOC stock. Because the decrease in total SOC is greater than the increase in vegetation C, net ecosystem C stock decreases with permafrost degradation. At the end of this century, permafrost degradation would cumulatively decrease ΔNEP by 203.55 ± 156.39 (RCP 4.5) and 325.67 ± 132.76 (RCP 8.5) Tg C, and decrease total ecosystem C stock by 209.44 ± 158.76 (RCP 4.5) and 371.06 ± 175.17 (RCP 8.5) Tg C, respectively. However, it should be noted that the decrease in NEP and total ecosystem C stock is caused from the single effect of permafrost degradation. When all factors are considered, including the effects of changing climate, increasing CO_2 , and thawing permafrost, permafrost regions of the QTP would still sequester more C in this century (Figure S3 in Supporting Information S1).

3.3. Responses of C Balance to ALT Deepening in Different Ecosystems

The effects of ALT deepening on C balance of the QTP show an obvious spatial heterogeneity (Figure 5). The eastern and southern parts of the permafrost regions on the QTP would increase more in both C pools and fluxes than the northwestern part due to ALT deepening, and the spatial heterogeneity is more noticeable under the RCP 8.5 than RCP 4.5. Given that the eastern and southern parts of the permafrost regions on the QTP are dominated by alpine meadow ecosystems, and the northwestern part is dominated by alpine steppe ecosystems (Figure 1), these results suggest that ALT deepening has greater influence on C balance of alpine meadows than alpine steppes, particularly under the RCP 8.5. However, changes in regional average ALT of these two ecosystems (Figure 6) show that the increase in ALT is smaller in alpine meadows. Therefore, C storage and fluxes of alpine meadows are more sensitive to ALT deepening than that of alpine steppes.

Under both RCPs and both ecosystems, the increase in ΔRH is greater than ΔNPP (Figure 6), and total SOC stocks in active layer and permafrost (ΔSOC_{NET}) decrease with ALT deepening (Figure 6), indicating that the net effects of ALT deepening would weaken ecosystem C sequestration in both ecosystems.

When comparing the two types of ecosystems, C sequestration weakening due to the single effect of permafrost degradation tends to be stronger in alpine steppe ecosystems. The cumulative difference in NEP between S_T and S_R from 2020 to 2099 are -77.94 ± 70.98 (RCP 4.5) and -144.03 ± 81.77 (RCP 8.5) Tg C for alpine meadows, and -115.14 ± 120.84 (RCP 4.5) and -157.07 ± 47.61 (RCP 8.5) Tg C for alpine steppes, respectively. The decreases in ΔSOC_{NET} are -85.32 ± 65.48 (RCP 4.5) and -182.97 ± 87.65 (RCP 8.5) Tg C for alpine meadows, and -121.62 ± 108.39 (RCP 4.5) and -176.81 ± 50.13 (RCP 8.5) Tg C for alpine steppes. However, given that the increase in ALT in alpine steppes is about twice as much as that in alpine meadows (Figure 6), C sequestration could reduce more in alpine meadows than alpine steppes with the same degree of ALT deepening.

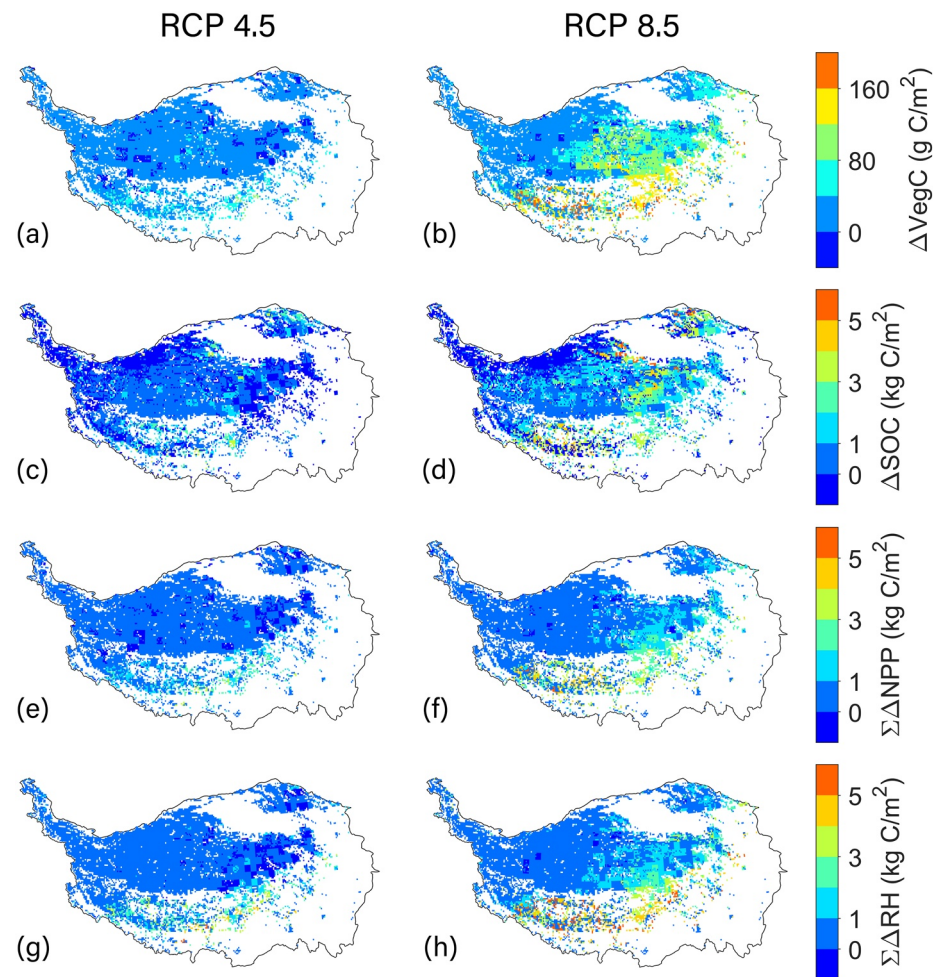


Figure 5. Changes in C balance of the QTP due to permafrost degradation under the RCP 4.5 and RCP 8.5. Δ before vegetation C (VegC) and SOC mean the difference between the results of the transient simulation and referenced simulation ($S_T - S_R$) in 2099, and Σ denotes the accumulation of each C flux from 2020 to 2099.

4. Discussion

4.1. Comparison With Other Studies

The estimated NPP, RH, and NEP of the permafrost region on the QTP during 2006–2011 were 194.2, 179.2, and 17.4 g C/m²/yr, respectively, all within the range of other estimates (120.8–329.6 g C/m²/yr for NPP, 149.8–303.5 g C/m²/yr for RH, and 4.0–26.1 g C/m²/yr for NEP; Table 1).

Existing studies show large differences in future C dynamics in the region (Table 1). Our estimation of flux density is higher than Z. Jin et al. (2015) but lower than Bosch et al. (2017) and Wei et al. (2021). RH estimation of Bosch et al. (2017) depends only on annual precipitation, which may induce large uncertainties in their future projection because important factors like soil temperature and SOC quality and quantity were not considered. Thawing-induced CO₂ emissions are also considered in the study of Bosch et al. (2017). However, the potential C loss from thawing permafrost was estimated from incubation experiments using soil samples from the arctic region. SOC density on the QTP (14.4–17.5 kg/m² for alpine meadows and 6.6–7.7 kg/m² for alpine steppes in 0–2 m; Mu et al., 2020) can be substantially lower than that in the arctic (55.1 ± 18.9 kg/m² for lowlands and 40.6 ± 22.7 kg/m² for uplands in upper one-m layer of the North American Arctic; Ping et al., 2008), which may cause an overestimate of RH in Bosch et al. (2017). Z. Jin et al. (2015) projected lower NPP and NEP in the 2090s under the RCP 8.5. TEM used in Z. Jin et al. (2015) was mainly calibrated for wetland ecosystems. Under the high warming scenario of the RCP 8.5, warming-induced high evapotranspiration may result

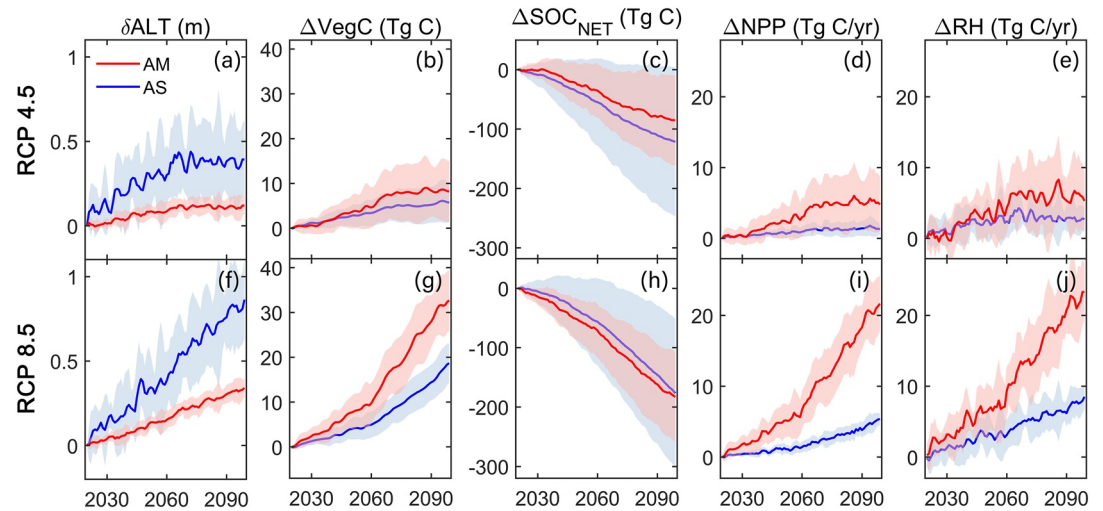


Figure 6. Anomalies of ALT from 2020 baseline and the effects of ALT deepening on ecosystem C balance of alpine meadow (AM) and alpine steppe (AS) ecosystems under the RCP 4.5 and RCP 8.5 scenarios. δ before ALT means the anomalies of ALT from 2020 baseline, and Δ before C balance components mean the differences between the results of the transient simulation and referenced simulation ($S_T - S_R$). ΔSOC_{NET} subtracts exposed permafrost C from ΔSOC to indicate the change of total SOC in active layer and permafrost due to permafrost degradation. Red and blue shade denote the standard deviation among all GCMs for alpine meadow and alpine steppe ecosystems, respectively.

Table 1

Estimated Regional C Fluxes on the QTP From Different Studies

| Model | Period | NPP | | RH | | NEP | | Source |
|-----------------|-------------------------|-------|---------|-------|---------|-------|---------|----------------------|
| | | Total | Density | Total | Density | Total | Density | |
| CENTURY | 1901–2010 | 344.0 | 244.7 | 336.5 | 239.0 | 7.5 | 5.3 | Lin et al. (2017) |
| TEM | 1961–2010 | 193.0 | 193.7 | 182.9 | 183.7 | 10.1 | 10.0 | Yan et al. (2015) |
| ORCHIDEE | 1961–2009 | 219.8 | 158.1 | 208.2 | 149.8 | 11.6 | 8.3 | Piao et al. (2012) |
| CASA | 1982–2009 | 177.2 | 120.8 | | | | | Zhang et al. (2014) |
| ORCHIDEE | 1980–2010 | 323.9 | 233.0 | | | | | Tan et al. (2010) |
| DOS-TEM | 1981–2012 | | 199.0 | | 195.0 | | 4.0 | Yi et al. (2014) |
| TEM | 1990s | 451.6 | 329.6 | 415.8 | 303.5 | 35.8 | 26.1 | Zhuang et al. (2010) |
| RG ¹ | 20,50 ³ | | | | 388.6 | | | Bosch et al. (2017) |
| | 20,50 ⁴ | | | | 391.2 | | | |
| | 20,70 ³ | | | | 385.9 | | | |
| | 20,70 ⁴ | | | | 389.2 | | | |
| LPJ-WHyMe | 2000–2018 | | | | | 152.4 | | Wei et al. (2021) |
| | 2090s ³ | | | | | 178.1 | | |
| | 2090s ⁴ | | | | | 317.9 | | |
| TEM | 2006–2011 | | 170.9 | | 160.5 | | 10.4 | Z. Jin et al. (2015) |
| | 2090s ³ | | 231.8 | | 198.7 | | 33.1 | |
| | 2090s ⁴ | | 252.5 | | 233.0 | | 19.5 | |
| TEM (S_T) | 2006–20,11 ³ | 188.3 | 194.2 | 171.4 | 179.2 | 16.8 | 17.4 | This study |
| | 2090s ³ | 237.0 | 241.3 | 219.6 | 226.4 | 17.2 | 15.0 | |
| | 2090s ⁴ | 319.3 | 317.4 | 264.9 | 269.9 | 55.9 | 50.1 | |

Note. Units for regional total C fluxes are Tg C/yr, and units for regional mean flux density are g C/m²/yr. 1. RG denotes regression model; 2, 3, and 4 represent estimations derived from the RCP 2.6, RCP 4.5, and RCP 8.5, respectively.

in water stress and suppress NPP for wetland ecosystems. In this study, TEM has been calibrated with the main ecosystems on the QTP, including alpine meadow, alpine steppe, alpine shrubland, and alpine desert ecosystems. Different calibrations should partially contribute to the differences in those projections. The differences in C sink strength projected by Wei et al. (2021) and this study can be partly attributed to the different study domains. Only the permafrost regions were focused on in this study, other than the entire QTP studied by Wei et al. (2021). Large areas of alpine shrubs, alpine meadows, and marshlands with strong C sequestration ability in nonpermafrost regions were excluded in this study, resulting in lower estimation than Wei et al. (2021). When comparing the studies of Z. Jin et al. (2015) and Wei et al. (2021), both of which studied the entire QTP, there are still large differences in their projections. The different model initial conditions, parameters, and model structures, such as the representations of soil thermal dynamics and the response of GPP to atmospheric CO₂ fertilization, may contribute to the variation in their projections (Koven et al., 2013; McGuire et al., 2016). However, although there are large differences in the magnitude of the projected NEP, all the studies predicted a stronger C sink strength of the QTP in the future.

4.2. Impact of Climate Change on Ecosystem C Balance

Although permafrost degradation contributes a fraction to the overall changes in C balance (Figure 4), the close relationship between S_T and S_R shows that climate change is still the main factor controlling ecosystem C balance (Figure S3 in Supporting Information S1). By 2099, ecosystem C storage and NEP of the permafrost region on the QTP would increase by 2.61 ± 0.58 Pg C and 0.46 ± 2.41 Tg C/yr under the RCP 4.5 and 5.11 ± 0.53 Pg C and 41.09 ± 6.28 Tg C/yr under the RCP 8.5, respectively. Six earth system models from phase five of the Coupled Model Inter-comparison Project (CMIP5) that did not consider the effects of permafrost degradation on SOC stocks show that NPP and RH increase from 1850 to 2100, and the C sink of the QTP would be higher during 2006–2100 in comparison with 1850–2005 under RCP4.5 scenario (S. Li et al., 2015). Increasing net nitrogen mineralization rate enhanced N availability, together with warming air temperature and rising CO₂ concentrations, promoting the regional C sink on the QTP (Zhuang et al., 2010).

In the northern high latitudes, warming and elevated atmospheric CO₂ concentration have been found as key drivers to NPP and RH dynamics, but precipitation changes are less important (McGuire et al., 2018). In contrast, on the QTP, air temperature, precipitation, and atmospheric CO₂ concentration in permafrost regions would all increase under both the RCPs (Figure S4 in Supporting Information). Evidence from experimental warming (Ganjurjav et al., 2016; J. Zhao et al., 2019), model simulation (Zheng et al., 2020), and meta-analysis (G. Wang et al., 2019) all suggest that C exchange in alpine meadows is mainly regulated by air temperature, but C exchange in dry alpine steppes is dominated by water conditions. Given the wide coverage of alpine steppes (7.2×10^5 km²; Wei et al., 2021) on the QTP, increment in precipitation should also be associated with C exchanges in the permafrost regions (Wei et al., 2021) as warming and elevated atmospheric CO₂ concentration (B. Chen et al., 2014; Piao et al., 2012) do. C dynamics responses on the QTP can be different from the conclusion of McGuire et al. (2018) for northern permafrost regions.

4.3. Nitrogen Subsidies From Permafrost Degradation

Permafrost degradation will not only release old C but also supply additional nitrogen that can be utilized to boost plant productivity. The direct effects of permafrost thaw would increase vegetation C storage and enhance C cycling on the QTP in the remaining of this century (Figure 3). Our analysis suggests that N subsidies from permafrost degradation should be the main reason for these increases in C storage and fluxes. When considering N addition during 2020–2099, SON experiences a remarkable surge in S_T (Figure 7; 49.87 ± 43.33 [RCP 4.5] and 122.18 ± 16.89 [RCP 8.5] Tg N) and shifts from a slight decrease in S_R (-0.48 ± 0.75 [RCP 4.5] and -1.92 ± 1.21 [RCP 8.5] Tg N) to a large amount of increase in S_T . The increase of N availability accumulatively enhances plant N uptake ($\Sigma(S_T - S_R)$: 8.68 ± 7.12 [RCP 4.5] and 21.38 ± 11.77 [RCP 8.5] Tg N) and makes plant gain more N ($S_T - S_R$: 0.58 ± 0.40 [RCP 4.5] and 1.68 ± 0.71 [RCP 8.5] Tg N), which, therefore, stimulates plant growth and increases NPP.

However, although both vegetation N and SON benefit from permafrost thaw, the increase in vegetation N is much smaller than in SON (Figure 7). Based on soil C and N balance, this study estimated that 0.61 ± 0.26 and 1.50 ± 0.15 Pg C of SOC, and 60.24 ± 32.37 and 127.68 ± 17.72 Tg N of SON would be added to active layer

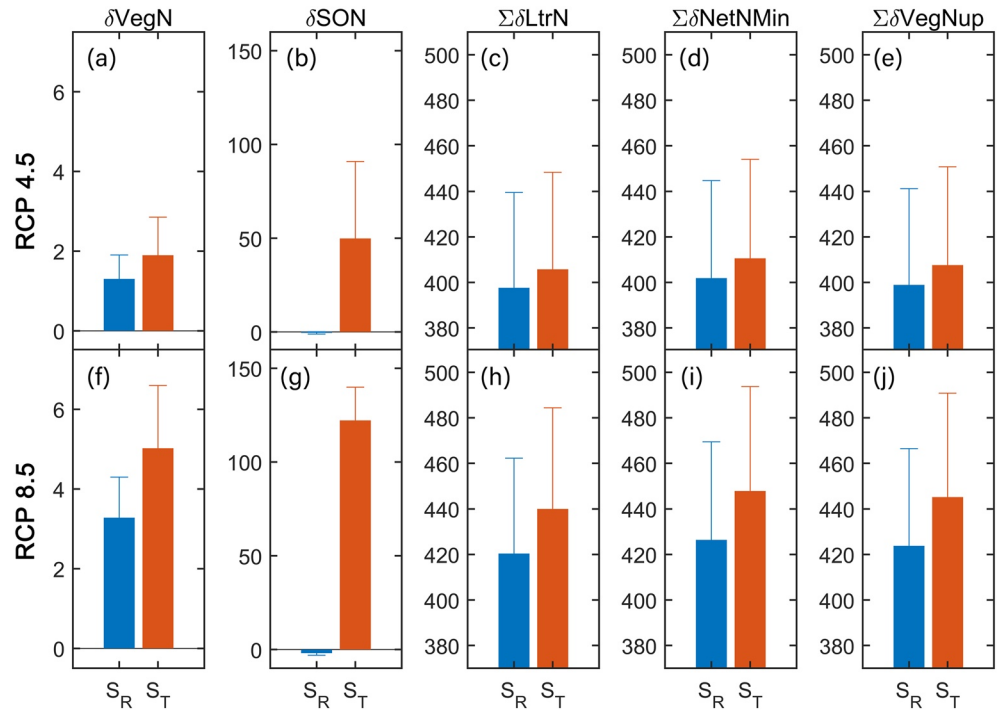


Figure 7. Changes in ecosystem N balance from 2020 baseline for the referenced simulation (S_R) and transient simulation (S_T) under the RCP 4.5 and RCP 8.5 scenarios. δ means the anomalies of N pools of 2099 from 2020 baseline; Σ denotes the accumulation of each N flux from 2020 to 2099. The error bars represent the standard deviation among all GCMs. Units for N pools (vegetation N [VegN] and soil organic N [SON]) are Tg N, and units for N fluxes (litter N [LtrN], net N mineralization [NetNMin], and vegetation N uptake [VegNup]) are Tg N/yr.

due to permafrost thaw (Table 2), under the RCP 4.5 and RCP 8.5, respectively. Among them, 22%–24% of these additional C would be decomposed through RH. However, only 12%–15% of these addition N would be absorbed by plants.

Figure S5 in Supporting Information S1, shows that N subsidies from permafrost thaw only alleviate plant N limit slightly. We find that although there is a large amount of N added to active layer due to permafrost thaw, only a small fraction of the amount can be accessed by plants. The average maximum rooting depth in permafrost regions on the QTP is estimated as 1.2 m, while the average ALT would increase to 2.9 ± 0.1 and 3.2 ± 0.1 m under the RCP 4.5 and RCP 8.5, respectively (Figure 4a), which is much greater than rooting zone depth. Therefore, only a small fraction of N released from thawed permafrost is absorbed by plants. The benefit of permafrost thaw is limited, but the consequence of permafrost thaw to C emission is significant. As a result, the net effects

Table 2
Changes in Soil C and N Balance Due To Permafrost Thaw

| C | ΔSOC | $\Sigma\Delta\text{LtrC}$ | $\Sigma\Delta\text{RH}$ | SOC_{PF} | $(\Sigma\Delta\text{RH} - \Sigma\Delta\text{LtrC})/\text{SOC}_{\text{PF}}$ |
|---------|--------------------|---------------------------|------------------------------|--------------------------|--|
| RCP 4.5 | 0.61 ± 0.26 | 0.33 ± 0.27 | 0.56 ± 0.44 | 0.84 ± 0.41 | 0.24 ± 0.15 |
| RCP 8.5 | 1.50 ± 0.15 | 0.81 ± 0.43 | 1.24 ± 0.62 | 1.93 ± 0.31 | 0.22 ± 0.07 |
| N | ΔSON | $\Sigma\Delta\text{LtrN}$ | $\Sigma\Delta\text{NetNMin}$ | SON_{PF} | $\Sigma\Delta\text{VegNup}/\text{SON}_{\text{PF}}$ |
| RCP 4.5 | 60.24 ± 32.37 | 8.11 ± 6.72 | 8.70 ± 7.23 | 60.83 ± 28.27 | 0.12 ± 0.10 |
| RCP 8.5 | 127.68 ± 17.72 | 19.60 ± 11.06 | 21.47 ± 11.87 | 129.55 ± 16.06 | 0.15 ± 0.06 |

Note. Δ means the differences between the transient simulation and referenced simulation ($S_T - S_R$); $\Sigma\Delta$ means the cumulative of $S_T - S_R$ from 2020 to 2099; SOC_{PF} and SON_{PF} mean SOC, and SON added to active layers from permafrost thaw, respectively. LtrC, LtrN, NetNMin, and VegNup denote litter C, litter N, net N mineralization, and vegetation N uptake, respectively. $(\Sigma\Delta\text{RH} - \Sigma\Delta\text{LtrC})$ is the part of thawing permafrost C that consumed by microbes. Units for C and N variables are Pg C and Tg N, respectively.

of permafrost thaw on the QTP are to weaken C sequestration. Similar results have also been found over the circumpolar permafrost regions. Permafrost thaw from 1970 to 2006 exposed 11.6 Pg C of SOC to decomposition, resulting in 4.03 Pg C emission but only 0.3 Pg C compensated by the stimulated plant C uptake (Hayes et al., 2014). In the forests of Northern Eurasia, the gain of vegetation C that is benefited from N supply due to permafrost degradation is only 29.8% (RCP4.5) to 49.2% (RCP8.5) of the loss of soil organic C. Permafrost degradation overall diminishes C sequestration in these forests (Kicklighter et al., 2019). Although N released from newly thawed permafrost can be used to stimulate plant productivity, plants may not be N limited or may not have access to them (Koven, Lawrence et al., 2015). However, new released SOC will be decomposed, although part of them take a longer time. Consequently, the stimulated RH may overwhelm the NPP increase (due to more available N to plant from thawing permafrost), decreasing the regional C sequestration.

There are several reasons for the limited access of plants to N released from permafrost degradation on the QTP. First, ALT (greater than two m; Ni et al., 2021; T. Wang et al., 2020; X. B. Wu et al., 2018) on the QTP is much deeper than rooting depth (generally smaller than 30 cm; Y. Yang et al., 2009) at present. N released from further deep permafrost in the future, therefore, could be far beyond plant accessibility if there are no substantial changes in plant species. Second, N mineralization in permafrost soils on the QTP has been found largely regulated by microbial traits (Mao et al., 2020; Zhang et al., 2020). Microbial biomass in permafrost on the QTP is 91.3% lower than that in active layer soils (Mao et al., 2020). The low abundance of microbes can become a key restriction on N mineralization after permafrost thaw, because of the direct role that microbes play in N transformation (Schimel & Bennett, 2004) and the positive effects of the extracellular enzymes (Ali et al., 2021; Luo et al., 2017) and microbial biomass (Z. L. Li et al., 2019; H. Wu et al., 2021) on soil N mineralization. Apart from microbial biomass, the higher abundance of bacteria than fungi in QTP permafrost may also have negative impacts on net N mineralization processes (Mao et al., 2020), because of the significantly higher metabolic N-demand and immobilization in bacteria than fungi (Kooijman et al., 2016). Further, the phase lag of heat transfer into deep soils can shift the deep soil organic matter mineralization later into fall and winter, producing a seasonal offset from the peak period of N demand during spring and summer (Koven, Lawrence et al., 2015), and reducing the access of plant to the additional N released from deep permafrost thaw. The remaining large fraction of N that cannot be used by plants could leach into aquatic ecosystems, causing far-reaching consequences on their functions and structure (Guo et al., 2019; Wickland et al., 2018), or could be lost via gaseous form of N_2O through nitrification and denitrification processes (Elberling et al., 2010; Voigt et al., 2017, 2020; Wilkerson et al., 2019), intensifying noncarbon feedback to climate warming (IPCC, 2013; Xu et al., 2012; G. Yang et al., 2018). Considering the serious consequences and the large amount of these additional N, sufficient attention should be paid to their fate on the QTP.

4.4. Nitrogen Subsidy Regimes From ALT Deepening in Different Ecosystems

The more pronounced influences of ALT deepening on C balance in alpine meadows than alpine steppes on the QTP can be partly due to different C and N subsidies from permafrost thaw. Although the increase in ALT is smaller in alpine meadows compared to alpine steppes, alpine meadows gain more C and N (Figures 6 and Figure 8). The maximum rooting depth of alpine meadow and alpine steppe ecosystems range from 0.5 to 1.9 m, but the average ALT in alpine meadows (2.15 ± 0.02 m) is shallower than alpine steppes (2.89 ± 0.07 m) at present. Although ALT increases more in alpine steppes, it mainly occurs in deep soils far below rooting zone. Therefore, only very limited N released from thawed permafrost can be accessed by alpine steppes. On the contrary, owing to the shallower ALT in alpine meadows, more N released from thawed permafrost is within its rooting zone, thus can be used. The addition of SOC and SON released from permafrost degradation in these two ecosystems (Table 3) support such explanations.

In addition, SOC and total nitrogen stocks in alpine meadows are about twice of that in alpine steppes on the QTP (Ding et al., 2016; L. Zhao et al., 2018), which may result in a significant increase in available C and N pools in alpine meadow ecosystem even with smaller increases in ALT. The higher density of SOC underneath alpine meadows can provide more substrates for microbe than that underneath alpine steppes, triggering a stronger RH response (Crowther et al., 2016). More SOC can also stimulate microbial activities and increase microbial biomass in alpine ecosystems (Y. Li et al., 2019), strengthening RH. Apart from quantity, incubation experiments found that SOM under alpine meadows is highly decomposable (L. Chen et al., 2016), while SOM under alpine

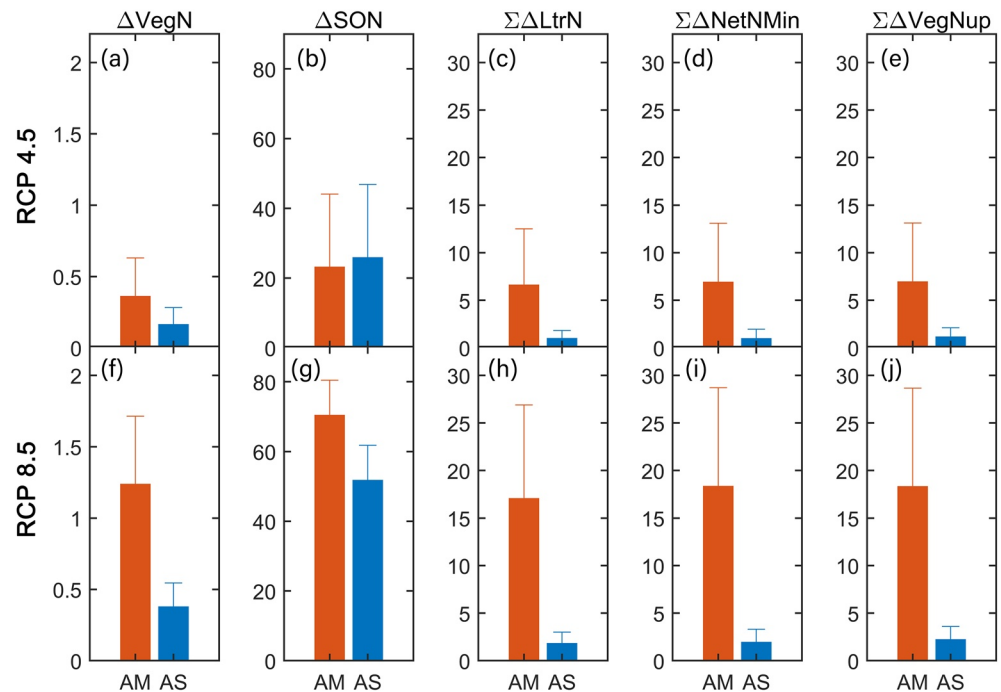


Figure 8. Differences in N balance between alpine meadow (AM) and alpine steppe (AS) ecosystems due to ALT deepening. Δ means the simulation differences between the transient simulation and referenced simulation ($S_T - S_R$) in 2099; Σ denotes the accumulative differences in N fluxes from 2020 to 2099. The error bars represent standard deviations among all GCMs. Units for N pools (vegetation N [VegN] and soil organic N [SON]) are Tg N, and units for N fluxes (litter N [LtrN], net N mineralization [NetNMin], and vegetation N uptake [VegNup]) are Tg N/yr.

steppes is largely composed of stable organic compounds (X. Wu et al., 2014). These differences may also contribute to a more sensitive RH in alpine meadow ecosystems (Eberwein et al., 2015).

The stronger response of Δ NPP to ALT in alpine meadows can partly be explained by the significantly higher usage of N supplied by permafrost thaw (Table 3). More than 25% of additional N is utilized in alpine meadows, while only less than 3% is absorbed by alpine steppes, therefore, contributing to distinct vegetation responses in Δ NPP. Alpine meadow ecosystem is mainly distributed in the eastern QTP. Relatively adequate precipitation, but also cold climate makes alpine meadows have higher soil water content than alpine steppes, which is distributed in arid climate. High soil water content in alpine meadows can facilitate N utilization by plants as water availability influences the diffusion of soil N to plant (Humbert et al., 2016; Simkin et al., 2016). Conversely, water limitation in alpine steppes constrain its nutrient availability and make it respond differently to climate warming and nitrogen addition from alpine meadows (Ganjurjav et al., 2016; S. Li et al., 2019; Zheng et al., 2020). Different water conditions in these two ecosystems may result in distinct differences in N usage (Table 3) and fluxes (Figure 8).

Table 3
Changes in SOC and SON in Alpine Meadow and Alpine Steppe Ecosystems Due To Permafrost Thaw

| C | Alpine meadow | | Alpine steppe | |
|---------|-------------------|-----------------------|-------------------|-----------------------|
| | SOC _{PF} | $\Sigma\Delta$ RH | SOC _{PF} | $\Sigma\Delta$ RH |
| RCP 4.5 | 0.48 ± 0.16 | 0.33 ± 0.28 | 0.36 ± 0.18 | 0.19 ± 0.18 |
| RCP 8.5 | 1.21 ± 0.16 | 0.85 ± 0.48 | 0.69 ± 0.11 | 0.31 ± 0.14 |
| N | Alpine meadow | | Alpine steppe | |
| | SON _{PF} | $\Sigma\Delta$ VegNup | SON _{PF} | $\Sigma\Delta$ VegNup |
| RCP 4.5 | 30.34 ± 11.64 | 6.99 ± 6.13 | 29.91 ± 16.94 | 1.19 ± 0.92 |
| RCP 8.5 | 73.14 ± 8.80 | 18.36 ± 10.30 | 55.60 ± 10.60 | 2.26 ± 1.34 |

Note. $\Sigma\Delta$ means the cumulative difference between the transient simulation and referenced simulation ($S_T - S_R$) from 2020 to 2099; SOC_{PF} and SON_{PF} mean SOC, and SON added to active layers from permafrost thaw, respectively. Units for soil C and N are Pg C and Tg N, respectively.

4.5. Study Limitations

Although the effects of exposed C and N from thawing permafrost were considered in TEM, it is still difficult to comprehensively evaluate the changes of terrestrial ecosystem C cycling under climate warming, due to the complex interactions between climate change, plant growth, microbe activities, hydrological and landscape dynamics, as well as human intervention. Some limitations of this study need further observational and modeling efforts to address.

First, this study assumed that rooting depth does not change over time, and available inorganic N released from thawing permafrost below rooting depth

is not accessible to plants. However, a recent experimental study (Blume-Werry et al., 2019) found that permafrost thaw led roots of some species to invade newly thawed permafrost and allow N uptake at depth. However, the effects of permafrost thaw on root growth varied between plant functional types. Rooting depth of dwarf shrubs showed a little response to permafrost thaw. Although ALT (greater than two m; Ni et al., 2021; T. Wang et al., 2020; X. B. Wu et al., 2018) on the QTP is much deeper than rooting depth (generally smaller than 30 cm; Y. Yang et al., 2009), observations and experiments on the changes of rooting depth of different species upon permafrost thaw can still benefit the quantification of ecosystem nutrient and C cycling under permafrost degradation.

Second, this study did not fully consider vegetation dynamics, such as plant species shift and distribution changes. Permafrost degradation on the QTP could reduce plant species and decrease the abundance of sedges but enrich forbs (X. Jin et al., 2020; Z. Yang et al., 2013). These changes in vegetation structure, distribution, as well as plant phenology could alter terrestrial ecosystem C cycling and should be considered in future studies.

Third, microbial colonization and a considerable increase in the diversity of microbial community upon permafrost thaw could significantly change soil C and N biogeochemical processes (Monteux et al., 2020). Coupling microbial community changes into modeling can better quantify soil C and N cycling in permafrost regions.

Furthermore, there are abundant lakes and wetlands on the QTP. Permafrost degradation, such as abrupt thaw, on the one hand, could form new lakes and wetlands to suppress C emissions in anaerobic environments, and on the other hand, could drain lakes and wetlands to strengthen C emissions by exposing waterlogged C to microbial decomposition (Schoor et al., 2015). Outburst of a headwater lake on the QTP may also accelerate the permafrost degradation surrounding the tailwater lake (Lu et al., 2020).

Finally, soil phosphorus availability should be taken into account in future studies. For example, a recent study on the QTP (G. Yang et al., 2021) found that changes in soil phosphorus availability play a critical role in regulating permafrost C cycle under climate warming.

5. Conclusions

We modified a process-based biogeochemistry model by considering the effects of extra carbon and nitrogen from thawing permafrost to quantify ecosystem C balance on the Qinghai-Tibetan plateau in the 21st century. Permafrost regions on the plateau would sequester more C and become a stronger C sink by the end of this century under both RCP 4.5 and RCP 8.5 scenarios. However, the single effect of permafrost degradation on the QTP is projected to diminish the ecosystem C sequestration capacity, because the increase in NPP stimulated by N supply from thawing permafrost is smaller than enhanced soil respiration. Due to the deep active layer on the QTP, N released from thawing permafrost is mainly distributed in deep soils, which is not accessible by plants, thus having a limited benefit to plant carbon uptake. As a result, the single effect of permafrost degradation would diminish ecosystem C sink by 209.44 ± 137.49 (RCP 4.5) and 371.06 ± 151.70 (RCP 8.5) Tg C during 2020–2099.

Permafrost degradation on the QTP has different effects on C balance of the distinct ecosystems of alpine meadow and alpine steppe. C storages and fluxes in alpine meadows respond more significantly to ALT deepening than that in alpine steppes, which could be due to the shallower ALT, the higher C and N stocks, and the wetter environment in alpine meadows.

Although more than 20% of the C released from thawing permafrost would be decomposed and emitted into the atmosphere, only less than 15% of the released N can be used by plants. The remaining large amount of N could have significant impacts on aquatic ecosystems and may intensify climate warming through another potent greenhouse gas N₂O release. Studies on this gas release shall draw sufficient attention on the plateau.

This study highlights the important effects of permafrost thaw on C and N cycling in permafrost dominated ecosystems and underscores the critical role of factoring deep permafrost carbon into land surface modeling in order to make more reliable projections of future permafrost carbon-climate feedbacks.

Conflict of Interest

The authors declare no conflict of interest relevant to this study.

Data Availability Statement

The model output and codes for data analysis in this study are available at Purdue University Research Repository (<https://purr.purdue.edu/publications/3867/1>).

Acknowledgments

This study is funded by the Second Tibetan Plateau Scientific Expedition and Research Program (2019QZKK0403), National Natural Science Foundation of China (41571193), and the “Strategic Priority Research Program” of the Chinese Academy of Sciences (XDA20020202). The authors thank two anonymous reviewers for their insightful comments and suggestions. The authors gratefully acknowledge financial support from China Scholarship Council. The authors also thank the ISIMIP cross sectoral science team for their roles in producing, coordinating, and making available the ISIMIP2b data (available at <https://esg.pik-potsdam.de/search/isimip/>).

References

- Abbott, B. W., Jones, J. B., Schuur, E. A. G., Chapin, F. S., Iii, Bowden, W. B., Bret-Harte, M. S., et al. (2016). Biomass offsets little or none of permafrost carbon release from soils, streams, and wildfire: An expert assessment. *Environmental Research Letters*, *11*(3), 034014. <https://doi.org/10.1088/1748-9326/11/3/034014>
- Ali, S., Dongchu, L., Jing, H., Ahmed, W., Abbas, M., Qaswar, M., et al. (2021). Soil microbial biomass and extracellular enzymes regulate nitrogen mineralization in a wheat-maize cropping system after three decades of fertilization in a Chinese ferrosol. *Journal of Soils and Sediments*, *21*(1), 281–294. <https://doi.org/10.1007/s11368-020-02770-5>
- Blume-Werry, G., Milbau, A., Teuber, L. M., Johansson, M., & Dorrepaal, E. (2019). Dwelling in the deep – Strongly increased root growth and rooting depth enhance plant interactions with thawing permafrost soil. *New Phytologist*, *223*(3), 1328–1339. <https://doi.org/10.1111/nph.15903>
- Bosch, A., Schmidt, K., He, J.-S., Doerfer, C., & Scholten, T. (2017). Potential CO₂ emissions from defrosting permafrost soils of the Qinghai-Tibet plateau under different scenarios of climate change in 2050 and 2070. *Catena*, *149*, 221–231. <https://doi.org/10.1016/j.catena.2016.08.035>
- Burke, E. J., Ekici, A., Huang, Y., Chadburn, S. E., Huntingford, C., Ciais, P., et al. (2017). Quantifying uncertainties of permafrost carbon-climate feedbacks. *Biogeosciences*, *14*(12), 3051–3066. <https://doi.org/10.5194/bg-14-3051-2017>
- Burke, E. J., Jones, C. D., & Koven, C. D. (2013). Estimating the permafrost-carbon climate response in the cmip5 climate models using a simplified approach. *Journal of Climate*, *26*(14), 4897–4909. <https://doi.org/10.1175/JCLI-D-12-00550.1>
- Chen, B., Zhang, X., Tao, J., Wu, J., Wang, J., Shi, P., et al. (2014). The impact of climate change and anthropogenic activities on alpine grassland over the Qinghai-Tibet plateau. *Agricultural and Forest Meteorology*, *189–190*, 11–18. <https://doi.org/10.1016/j.agrformet.2014.01.002>
- Chen, L., Liang, J., Qin, S., Liu, L., Fang, K., Xu, Y., et al. (2016). Determinants of carbon release from the active layer and permafrost deposits on the Tibetan plateau. *Nature Communications*, *7*(1), 13046. <https://doi.org/10.1038/ncomms13046>
- Crowther, T. W., Todd-Brown, K. E. O., Rowe, C. W., Wieder, W. R., Carey, J. C., Machmuller, M. B., et al. (2016). Quantifying global soil carbon losses in response to warming. *Nature*, *540*(7631), 104–108. <https://doi.org/10.1038/nature20150>
- Ding, J., Chen, L., Ji, C., Hugelius, G., Li, Y., Liu, L., et al. (2017). Decadal soil carbon accumulation across Tibetan permafrost regions. *Nature Geoscience*, *10*(6), 420–424. <https://doi.org/10.1038/ngeo2945>
- Ding, J., Li, F., Yang, G., Chen, L., Zhang, B., Liu, L., et al. (2016). The permafrost carbon inventory on the Tibetan plateau: A new evaluation using deep sediment cores. *Global Change Biology*, *22*(8), 2688–2701. <https://doi.org/10.1111/gcb.13257>
- Eberwein, J. R., Oikawa, P. Y., Allsman, L. A., & Jenerette, G. D. (2015). Carbon availability regulates soil respiration response to nitrogen and temperature. *Soil Biology and Biochemistry*, *88*, 158–164. <https://doi.org/10.1016/j.soilbio.2015.05.014>
- Editorial Committee of Vegetation Map of China, Chinese Academy of Sciences. (2001). *Vegetation atlas of China*. Science Press.
- Elberling, B., Christiansen, H. H., & Hansen, B. U. (2010). High nitrous oxide production from thawing permafrost. *Nature Geoscience*, *3*(5), 332–335. <https://doi.org/10.1038/ngeo803>
- Farr, T. G., Rosen, P. A., Caro, E., Crippen, R., Duren, R., Hensley, S., et al. (2007). The shuttle radar topography mission. *Reviews of Geophysics*, *45*(2). <https://doi.org/10.1029/2005RG000183>
- Finger, R. A., Turetsky, M. R., Kielland, K., Ruess, R. W., Mack, M. C., & Euskirchen, E. S. (2016). Effects of permafrost thaw on nitrogen availability and plant-soil interactions in a boreal Alaskan lowland. *Journal of Ecology*, *104*(6), 1542–1554. <https://doi.org/10.1111/1365-2745.12639>
- Frieler, K., Lange, S., Piontek, F., Reyer, C. P. O., Schewe, J., Warszawski, L., et al. (2017). Assessing the impacts of 1.5 degrees C global warming - Simulation protocol of the inter-sectoral impact model intercomparison project (isimip2b). *Geoscientific Model Development*, *10*(12), 4321–4345. <https://doi.org/10.5194/gmd-10-4321-2017>
- Ganjurjav, H., Gao, Q. Z., Gornish, E. S., Schwartz, M. W., Liang, Y., Cao, X. J., et al. (2016). Differential response of alpine steppe and alpine meadow to climate warming in the central Qinghai-Tibetan plateau. *Agricultural and Forest Meteorology*, *223*, 233–240. <https://doi.org/10.1016/j.agrformet.2016.03.017>
- Guo, Y. D., Song, C. C., Tan, W. W., Wang, X. W., & Lu, Y. Z. (2019). Export of dissolved nitrogen in catchments underlain by permafrost in northeast China. *The Science of the Total Environment*, *660*, 1210–1218. <https://doi.org/10.1016/j.scitotenv.2018.12.464>
- Hao, A., Xue, X., Wang, X., Zhao, G., You, Q., Peng, F., et al. (2021). Different response of alpine meadow and alpine steppe to climatic and anthropogenic disturbance on the Tibetan plateau. *Global Ecology and Conservation*, *27*, e01512. <https://doi.org/10.1016/j.gecco.2021.e01512>
- Hayes, D. J., Kicklighter, D. W., McGuire, A. D., Chen, M., Zhuang, Q., Yuan, F., et al. (2014). The impacts of recent permafrost thaw on land-atmosphere greenhouse gas exchange. *Environmental Research Letters*, *9*(4), 045005. <https://doi.org/10.1088/1748-9326/9/4/045005>
- Hayes, D. J., McGuire, A. D., Kicklighter, D. W., Gurney, K. R., Burnside, T. J., & Melillo, J. M. (2011). Is the northern high-latitude land-based CO₂ sink weakening? *Global Biogeochemical Cycles*, *25*(3). <https://doi.org/10.1029/2010GB003813>
- Humbert, J. Y., Dwyer, J. M., Andrey, A., & Arlettaz, R. (2016). Impacts of nitrogen addition on plant biodiversity in mountain grasslands depend on dose, application duration and climate: A systematic review. *Global Change Biology*, *22*(1), 110–120. <https://doi.org/10.1111/gcb.12986>
- IPCC. (2013). In T. F. Stocker, D. Qin, G.-K. Plattner, M. Tignor, S. K. Allen, J. Boschung et al. (Eds.), *Climate change 2013: The physical science basis. Contribution of Working Group I the Fifth Assessment Report of the Intergovernmental Panel on Climate Change* (p. 1535). Cambridge University Press.
- Jin, X., Jin, H., Wu, X., Luo, D., Yu, S., Li, X., et al. (2020). Permafrost degradation leads to biomass and species richness decreases on the northeastern Qinghai-Tibet plateau. *Plants*, *9*(11), 1453. <https://doi.org/10.3390/plants9111453>
- Jin, Z., Zhuang, Q., He, J.-S., Luo, T., & Shi, Y. (2013). Phenology shift from 1989 to 2008 on the Tibetan plateau: An analysis with a process-based soil physical model and remote sensing data. *Climatic Change*, *119*(2), 435–449. <https://doi.org/10.1007/s10584-013-0722-7>
- Jin, Z., Zhuang, Q., He, J.-S., Zhu, X., & Song, W. (2015). Net exchanges of methane and carbon dioxide on the Qinghai-Tibetan plateau from 1979 to 2100. *Environmental Research Letters*, *10*(8), 085007. <https://doi.org/10.1088/1748-9326/10/8/085007>
- Jones, C. D., Arora, V., Friedlingstein, P., Bopp, L., Brovkin, V., Dunne, J., et al. (2016). C4MIP – The coupled climate-carbon cycle model intercomparison project: Experimental protocol for cmip6. *Geoscientific Model Development*, *9*(8), 2853–2880. <https://doi.org/10.5194/gmd-9-2853-2016>

- Keuper, F., van Bodegom, P. M., Dorrepaal, E., Weedon, J. T., van Hal, J., van Logtestijn, R. S. P., & Aerts, R. (2012). A frozen feast: Thawing permafrost increases plant-available nitrogen in subarctic peatlands. *Global Change Biology*, 18(6), 1998–2007. <https://doi.org/10.1111/j.1365-2486.2012.02663.x>
- Kicklighter, D. W., Melillo, J. M., Monier, E., Sokolov, A. P., & Zhuang, Q. (2019). Future nitrogen availability and its effect on carbon sequestration in northern Eurasia. *Nature Communications*, 10(1), 3024. <https://doi.org/10.1038/s41467-019-10944-0>
- Kooijman, A. M., Bloem, J., van Dalen, B. R., & Kalbitz, K. (2016). Differences in activity and n demand between bacteria and fungi in a microcosm incubation experiment with selective inhibition. *Applied Soil Ecology*, 99, 37–47. <https://doi.org/10.1016/j.apsoil.2015.11.011>
- Kou, D., Ding, J., Li, F., Wei, N., Fang, K., Yang, G., et al. (2019). Spatially-explicit estimate of soil nitrogen stock and its implication for land model across Tibetan alpine permafrost region. *The Science of the Total Environment*, 650, 1795–1804. <https://doi.org/10.1016/j.scitotenv.2018.09.252>
- Koven, C. D., Lawrence, D. M., & Riley, W. J. (2015). Permafrost carbon-climate feedback is sensitive to deep soil carbon decomposability but not deep soil nitrogen dynamics. *Proceedings of the National Academy of Sciences of the United States of America*, 112(12), 3752–3757. <https://doi.org/10.1073/pnas.1415123112>
- Koven, C. D., Riley, W. J., & Stern, A. (2013). Analysis of permafrost thermal dynamics and response to climate change in the CMIP5 earth system models. *Journal of Climate*, 26(6), 1877–1900. <https://doi.org/10.1175/jcli-d-12-00228.1>
- Koven, C. D., Ringeval, B., Friedlingstein, P., Ciais, P., Cadule, P., Khvorostyanov, D., et al. (2011). Permafrost carbon-climate feedbacks accelerate global warming. *Proceedings of the National Academy of Sciences*, 108(36), 14769–14774. <https://doi.org/10.1073/pnas.1103910108>
- Koven, C. D., Schuur, E. A. G., Schadel, C., Bohn, T. J., Burke, E. J., Chen, G., et al. (2015). A simplified, data-constrained approach to estimate the permafrost carbon-climate feedback. *Philosophical Transactions of the Royal Society A: Mathematical, Physical & Engineering Sciences*, 373(2054), 23. <https://doi.org/10.1098/rsta.2014.0423>
- Li, S., Dong, S., Shen, H., Han, Y., Zhang, J., Xu, Y., et al. (2019). Different responses of multifaceted plant diversities of alpine meadow and alpine steppe to nitrogen addition gradients on Qinghai-Tibetan plateau. *The Science of the Total Environment*, 688, 1405–1412. <https://doi.org/10.1016/j.scitotenv.2019.06.211>
- Li, S., Lü, S., Gao, Y., & Ao, Y. (2015). The change of climate and terrestrial carbon cycle over Tibetan Plateau in CMIP5 models. *International Journal of Climatology*, 35(14), 4359–4369. <https://doi.org/10.1002/joc.4293>
- Li, Y., Lv, W., Jiang, L., Zhang, L., Wang, S., Wang, Q., et al. (2019). Microbial community responses reduce soil carbon loss in Tibetan alpine grasslands under short-term warming. *Global Change Biology*, 25(10), 3438–3449. <https://doi.org/10.1111/gcb.14734>
- Li, Z. L., Tian, D. S., Wang, B. X., Wang, J. S., Wang, S., Chen, H. Y. H., et al. (2019). Microbes drive global soil nitrogen mineralization and availability. *Global Change Biology*, 25(3), 1078–1088. <https://doi.org/10.1111/gcb.14557>
- Liang, J., Xia, J., Shi, Z., Jiang, L., Ma, S., Lu, X., et al. (2018). Biotic responses buffer warming-induced soil organic carbon loss in arctic tundra. *Global Change Biology*, 24(10), 4946–4959. <https://doi.org/10.1111/gcb.14325>
- Lin, X., Han, P., Zhang, W., & Wang, G. (2017). Sensitivity of alpine grassland carbon balance to interannual variability in climate and atmospheric CO₂ on the Tibetan plateau during the last century. *Global and Planetary Change*, 154, 23–32. <https://doi.org/10.1016/j.gloplacha.2017.05.008>
- Liu, Y., Geng, X., TenzintarchenWei, D., Dai, D., & Xu, R. (2020). Divergence in ecosystem carbon fluxes and soil nitrogen characteristics across alpine steppe, alpine meadow and alpine swamp ecosystems in a biome transition zone. *The Science of the Total Environment*, 748, 142453. <https://doi.org/10.1016/j.scitotenv.2020.142453>
- Lu, P., Han, J., Li, Z., Xu, R., Li, R., Hao, T., & Qiao, G. (2020). Lake outburst accelerated permafrost degradation on Qinghai-Tibet plateau. *Remote Sensing of Environment*, 249, 112011. <https://doi.org/10.1016/j.rse.2020.112011>
- Luo, L., Meng, H., & Gu, J. D. (2017). Microbial extracellular enzymes in biogeochemical cycling of ecosystems. *Journal of Environmental Management*, 197, 539–549. <https://doi.org/10.1016/j.jenvman.2017.04.023>
- MacDougall, A. H., & Knutti, R. (2016). Projecting the release of carbon from permafrost soils using a perturbed parameter ensemble modelling approach. *Biogeosciences*, 13(7), 2123–2136. <https://doi.org/10.5194/bg-13-2123-2016>
- Mao, C., Kou, D., Chen, L., Qin, S., Zhang, D., Peng, Y., & Yang, Y. (2020). Permafrost nitrogen status and its determinants on the Tibetan plateau. *Global Change Biology*, 26(9), 5290–5302. <https://doi.org/10.1111/gcb.15205>
- McGuire, A. D., Koven, C., Lawrence, D. M., Clein, J. S., Xia, J. Y., Beer, C., et al. (2016). Variability in the sensitivity among model simulations of permafrost and carbon dynamics in the permafrost region between 1960 and 2009. *Global Biogeochemical Cycles*, 30(7), 1015–1037. <https://doi.org/10.1002/2016gb005405>
- McGuire, A. D., Lawrence, D. M., Koven, C., Clein, J. S., Burke, E., Chen, G. S., et al. (2018). Dependence of the evolution of carbon dynamics in the northern permafrost region on the trajectory of climate change. *Proceedings of the National Academy of Sciences of the United States of America*, 115(15), 3882–3887. <https://doi.org/10.1073/pnas.1719903115>
- McGuire, A. D., Melillo, J. M., Joyce, L. A., Kicklighter, D. W., Grace, A. L., Moore, B., & Vorosmarty, C. J. (1992). Interactions between carbon and nitrogen dynamics in estimating net primary productivity for potential vegetation in North America. *Global Biogeochemical Cycles*, 6(2), 101–124. <https://doi.org/10.1029/92gb00219>
- Mishra, U., Hugelius, G., Shelef, E., Yang, Y., Strauss, J., Lupachev, A., et al. (2021). Spatial heterogeneity and environmental predictors of permafrost region soil organic carbon stocks. *Science Advances*, 7(9), eaaz5236. <https://doi.org/10.1126/sciadv.aaz5236>
- Monteux, S., Keuper, F., Fontaine, S., Gavazov, K., Hallin, S., Juhanson, J., et al. (2020). Carbon and nitrogen cycling in Yedoma permafrost controlled by microbial functional limitations. *Nature Geoscience*, 13(12), 794–798. <https://doi.org/10.1038/s41561-020-00662-4>
- Moss, R. H., Edmonds, J. A., Hibbard, K. A., Manning, M. R., Rose, S. K., van Vuuren, D. P., et al. (2010). The next generation of scenarios for climate change research and assessment. *Nature*, 463(7282), 747–756. <https://doi.org/10.1038/nature08823>
- Mu, C., Abbott, B. W., Norris, A. J., Mu, M., Fan, C., Chen, X., et al. (2020). The status and stability of permafrost carbon on the Tibetan plateau. *Earth-Science Reviews*, 211, 103433. <https://doi.org/10.1016/j.earscirev.2020.103433>
- Ni, J., Wu, T., Zhu, X., Hu, G., Zou, D., Wu, X., et al. (2021). Simulation of the present and future projection of permafrost on the Qinghai-Tibet plateau with statistical and machine learning models. *Journal of Geophysical Research: Atmospheres*, 126(2), e2020JD033402. <https://doi.org/10.1029/2020JD033402>
- Peng, F., Xue, X., Li, C., Lai, C., Sun, J., Tsubo, M., et al. (2020). Plant community of alpine steppe shows stronger association with soil properties than alpine meadow alongside degradation. *The Science of the Total Environment*, 733, 139048. <https://doi.org/10.1016/j.scitotenv.2020.139048>
- Peng, X., Zhang, T., Frauenfeld, O. W., Wang, S., Qiao, L., Du, R., & Mu, C. (2020). Northern hemisphere greening in association with warming permafrost. *Journal of Geophysical Research: Biogeosciences*, 125(1), e2019JG005086. <https://doi.org/10.1029/2019jg005086>
- Piao, S., Tan, K., Nan, H., Ciais, P., Fang, J., Wang, T., et al. (2012). Impacts of climate and CO₂ changes on the vegetation growth and carbon balance of Qinghai-Tibetan grasslands over the past five decades. *Global and Planetary Change*, 98–99, 73–80. <https://doi.org/10.1016/j.gloplacha.2012.08.009>

- Ping, C.-L., Michaelson, G. J., Jorgenson, M. T., Kimble, J. M., Epstein, H., Romanovsky, V. E., & Walker, D. A. (2008). High stocks of soil organic carbon in the north American arctic region. *Nature Geoscience*, *1*(9), 615–619. <https://doi.org/10.1038/ngeo284>
- Qian, H. F., Joseph, R., & Zeng, N. (2010). Enhanced terrestrial carbon uptake in the northern high latitudes in the 21st century from the coupled carbon cycle climate model intercomparison project model projections. *Global Change Biology*, *16*(2), 641–656. <https://doi.org/10.1111/j.1365-2486.2009.01989.x>
- Qin, Y., Wu, T., Zhao, L., Wu, X., Li, R., Xie, C., et al. (2017). Numerical modeling of the active layer thickness and permafrost thermal state across Qinghai-Tibetan plateau. *Journal of Geophysical Research: Atmospheres*, *122*(2111), 604620–605611. <https://doi.org/10.1002/2017JD026858>
- Salmon, V. G., Schadel, C., Bracho, R., Pegoraro, E., Celis, G., Mauritz, M., et al. (2018). Adding depth to our understanding of nitrogen dynamics in permafrost soils. *Journal of Geophysical Research-Biogeosciences*, *123*(8), 2497–2512. <https://doi.org/10.1029/2018jg004518>
- Salmon, V. G., Soucy, P., Mauritz, M., Celis, G., Natali, S. M., Mack, M. C., & Schuur, E. A. G. (2016). Nitrogen availability increases in a tundra ecosystem during five years of experimental permafrost thaw. *Global Change Biology*, *22*(5), 1927–1941. <https://doi.org/10.1111/gcb.13204>
- Schaefer, K., Lantuit, H., Romanovsky, V. E., Schuur, E. A. G., & Witt, R. (2014). The impact of the permafrost carbon feedback on global climate. *Environmental Research Letters*, *9*(8), 085003. <https://doi.org/10.1088/1748-9326/9/8/085003>
- Schaphoff, S., Heyder, U., Ostberg, S., Gerten, D., Heinke, J., & Lucht, W. (2013). Contribution of permafrost soils to the global carbon budget. *Environmental Research Letters*, *8*(1), 014026. <https://doi.org/10.1088/1748-9326/8/1/014026>
- Schimel, J. P., & Bennett, J. (2004). Nitrogen mineralization: Challenges of a changing paradigm. *Ecology*, *85*(3), 591–602. <https://doi.org/10.1890/03-8002>
- Schuur, E. A. G., McGuire, A. D., Schadel, C., Grosse, G., Harden, J. W., Hayes, D. J., et al. (2015). Climate change and the permafrost carbon feedback. *Nature*, *520*(7546), 171–179. <https://doi.org/10.1038/nature14338>
- Shu, S., Jain, A. K., Koven, C. D., & Mishra, U. (2020). Estimation of permafrost soc stock and turnover time using a land surface model with vertical heterogeneity of permafrost soils. *Global Biogeochemical Cycles*, *34*(11), e2020GB006585. <https://doi.org/10.1029/2020GB006585>
- Simkin, S. M., Allen, E. B., Bowman, W. D., Clark, C. M., Belnap, J., Brooks, M. L., et al. (2016). Conditional vulnerability of plant diversity to atmospheric nitrogen deposition across the United States. *Proceedings of the National Academy of Sciences of the United States of America*, *113*(15), 4086–4091. <https://doi.org/10.1073/pnas.1515241113>
- Tan, K., Ciaï, P., Piao, S., Wu, X., Tang, Y., Vuichard, N., et al. (2010). Application of the ORCHIDEE global vegetation model to evaluate biomass and soil carbon stocks of Qinghai-Tibetan grasslands. *Global Biogeochemical Cycles*, *24*(1). <https://doi.org/10.1029/2009GB003530>
- Voigt, C., Marushchak, M. E., Abbott, B. W., Biasi, C., Elberling, B., Siciliano, S. D., et al. (2020). Nitrous oxide emissions from permafrost-affected soils. *Nature Reviews Earth & Environment*, *1*(8), 420–434. <https://doi.org/10.1038/s43017-020-0063-9>
- Voigt, C., Marushchak, M. E., Lamprecht, R. E., Jackowicz-Korczynski, M., Lindgren, A., Mastepanov, M., et al. (2017). Increased nitrous oxide emissions from arctic peatlands after permafrost thaw. *Proceedings of the National Academy of Sciences of the United States of America*, *114*(24), 6238–6243. <https://doi.org/10.1073/pnas.1702902114>
- Wang, G., Li, F., Peng, Y., Yu, J., Zhang, D., Yang, G., et al. (2019). Responses of soil respiration to experimental warming in an alpine steppe on the Tibetan plateau. *Environmental Research Letters*, *14*(9), 094015. <https://doi.org/10.1088/1748-9326/ab3bbc>
- Wang, L., Liu, H., Shao, Y., Liu, Y., & Sun, J. (2018). Water and co₂ fluxes over semiarid alpine steppe and humid alpine meadow ecosystems on the Tibetan plateau. *Theoretical and Applied Climatology*, *131*(1), 547–556. <https://doi.org/10.1007/s00704-016-1997-1>
- Wang, S. Y., Zhang, B., Yang, Q. C., Chen, G. S., Yang, B. J., Lu, L. L., et al. (2017). Responses of net primary productivity to phenological dynamics in the Tibetan plateau, China. *Agricultural and Forest Meteorology*, *232*, 235–246. <https://doi.org/10.1016/j.agrformet.2016.08.020>
- Wang, T. (2019). *Frozen ground map of China based on a map of the Glaciers, frozen ground and deserts in China*. National Cryosphere desert data center. Retrieved from <http://www.ncdc.ac.cn>
- Wang, T., Yang, D., Yang, Y., Piao, S., Li, X., Cheng, G., & Fu, B. (2020). Permafrost thawing puts the frozen carbon at risk over the Tibetan plateau. *Science Advances*, *6*(19), eaaz3513. <https://doi.org/10.1126/sciadv.aaz3513>
- Wei, D., Qi, Y., Ma, Y., Wang, X., Ma, W., Gao, T., et al. (2021). Plant uptake of CO₂ outpaces losses from permafrost and plant respiration on the Tibetan Plateau. *Proceedings of the National Academy of Sciences*, *118*(33), e2015283118. <https://doi.org/10.1073/pnas.2015283118>
- Wickland, K. P., Waldrop, M. P., Aiken, G. R., Koch, J. C., Jorgenson, M. T., & Striegl, R. G. (2018). Dissolved organic carbon and nitrogen release from boreal Holocene permafrost and seasonally frozen soils of Alaska. *Environmental Research Letters*, *13*(6), 065011. <https://doi.org/10.1088/1748-9326/aac4ad>
- Wieder, W. (2014). *Regridded harmonized world soil database v1.2*. ORNL Distributed Active Archive Center.
- Wilkerson, J., Dobosy, R., Sayres, D. S., Healy, C., Dumas, E., Baker, B., & Anderson, J. G. (2019). Permafrost nitrous oxide emissions observed on a landscape scale using the airborne eddy-covariance method. *Atmospheric Chemistry and Physics*, *19*(7), 4257–4268. <https://doi.org/10.5194/acp-19-4257-2019>
- Wu, H., Cai, A., Xing, T., Huai, S., Zhu, P., Xu, M., & Lu, C. (2021). Fertilization enhances mineralization of soil carbon and nitrogen pools by regulating the bacterial community and biomass. *Journal of Soils and Sediments*, *21*, 1633–1643. <https://doi.org/10.1007/s11368-020-02865-z>
- Wu, Q., Zhang, T., & Liu, Y. (2012). Thermal state of the active layer and permafrost along the Qinghai-Xizang (Tibet) railway from 2006 to 2010. *The Cryosphere*, *6*(3), 607–612. <https://doi.org/10.5194/tc-6-607-2012>
- Wu, X., Fang, H., Zhao, L., Wu, T., Li, R., Ren, Z., et al. (2014). Mineralization and changes in the fractions of soil organic matter in soils of the permafrost region, Qinghai-Tibet plateau, China. *Permafrost and Periglacial Processes*, *25*(1), 35–44. <https://doi.org/10.1002/ppp.1796>
- Wu, X. B., Nan, Z. T., Zhao, S. P., Zhao, L., & Cheng, G. D. (2018). Spatial modeling of permafrost distribution and properties on the Qinghai-Tibet plateau. *Permafrost and Periglacial Processes*, *29*(2), 86–99. <https://doi.org/10.1002/ppp.1971>
- Xu, R., Prentice, I. C., Spahni, R., & Niu, H. S. (2012). Modelling terrestrial nitrous oxide emissions and implications for climate feedback. *New Phytologist*, *196*(2), 472–488. <https://doi.org/10.1111/j.1469-8137.2012.04269.x>
- Yan, L., Zhou, G. S., Wang, Y. H., Hu, T. Y., & Sui, X. H. (2015). The spatial and temporal dynamics of carbon budget in the alpine grasslands on the Qinghai-Tibetan plateau using the terrestrial ecosystem model. *Journal of Cleaner Production*, *107*, 195–201. <https://doi.org/10.1016/j.jclepro.2015.04.140>
- Yang, G. B., Peng, Y. F., Abbott, B. W., Biasi, C., Wei, B., Zhang, D., et al. (2021). Phosphorus rather than nitrogen regulates ecosystem carbon dynamics after permafrost thaw. *Global Change Biology*, *27*(22), 5818–5830. <https://doi.org/10.1111/gcb.15845>
- Yang, G. B., Peng, Y. F., Marushchak, M. E., Chen, Y. L., Wang, G. Q., Li, F., et al. (2018). Magnitude and pathways of increased nitrous oxide emissions from uplands following permafrost thaw. *Environmental Science & Technology*, *52*(16), 9162–9169. <https://doi.org/10.1021/acs.est.8b02271>
- Yang, Y., Fang, J., Ji, C., & Han, W. (2009). Above- and belowground biomass allocation in Tibetan grasslands. *Journal of Vegetation Science*, *20*(1), 177–184. <https://doi.org/10.1111/j.1654-1103.2009.05566.x>

- Yang, Z., Gao, J., Zhao, L., Xu, X., & Ouyang, H. (2013). Linking thaw depth with soil moisture and plant community composition: Effects of permafrost degradation on alpine ecosystems on the Qinghai-Tibet plateau. *Plant and Soil*, 367(1), 687–700. <https://doi.org/10.1007/s11104-012-1511-1>
- Yi, S., Wang, X., Qin, Y., Xiang, B., & Ding, Y. (2014). Responses of alpine grassland on Qinghai-Tibetan plateau to climate warming and permafrost degradation: A modeling perspective. *Environmental Research Letters*, 9(7), 074014. <https://doi.org/10.1088/1748-9326/9/7/074014>
- Zhang, Y., Qi, W., Zhou, C., Ding, M., Liu, L., Gao, J., et al. (2014). Spatial and temporal variability in the net primary production of alpine grassland on the Tibetan plateau since 1982. *Journal of Geographical Sciences*, 24(2), 269–287. <https://doi.org/10.1007/s11442-014-1087-1>
- Zhang, Y., Zhang, N., Yin, J., Zhao, Y., Yang, F., Jiang, Z., et al. (2020). Simulated warming enhances the responses of microbial n transformations to reactive n input in a Tibetan alpine meadow. *Environment International*, 141, 105795. <https://doi.org/10.1016/j.envint.2020.105795>
- Zhao, J., Luo, T., Wei, H., Deng, Z., Li, X., Li, R., & Tang, Y. (2019). Increased precipitation offsets the negative effect of warming on plant biomass and ecosystem respiration in a Tibetan alpine steppe. *Agricultural and Forest Meteorology*, 279, 107761. <https://doi.org/10.1016/j.agrformet.2019.107761>
- Zhao, L., Wu, X. D., Wang, Z. W., Sheng, Y., Fang, H. B., Zhao, Y. H., et al. (2018). Soil organic carbon and total nitrogen pools in permafrost zones of the Qinghai-Tibetan plateau. *Scientific Reports*, 8, 1–9. <https://doi.org/10.1038/s41598-018-22024-2>
- Zheng, Z. T., Zhu, W. Q., & Zhang, Y. J. (2020). Seasonally and spatially varied controls of climatic factors on net primary productivity in alpine grasslands on the Tibetan plateau. *Global Ecology and Conservation*, 21, e00814. <https://doi.org/10.1016/j.gecco.2019.e00814>
- Zhu, Q., & Zhuang, Q. (2014). Parameterization and sensitivity analysis of a process-based terrestrial ecosystem model using adjoint method. *Journal of Advances in Modeling Earth Systems*, 6(2), 315–331. <https://doi.org/10.1002/2013MS000241>
- Zhuang, Q., He, J., Lu, Y., Ji, L., Xiao, J., & Luo, T. (2010). Carbon dynamics of terrestrial ecosystems on the Tibetan plateau during the 20th century: An analysis with a process-based biogeochemical model. *Global Ecology and Biogeography*, 19(5), 649–662. <https://doi.org/10.1111/j.1466-8238.2010.00559.x>
- Zhuang, Q., McGuire, A. D., Melillo, J. M., Klein, J. S., Dargaville, R. J., Kicklighter, D. W., et al. (2011). Carbon cycling in extratropical terrestrial ecosystems of the northern hemisphere during the 20th century: A modeling analysis of the influences of soil thermal dynamics. *Tellus B: Chemical and Physical Meteorology*, 55(3), 751–776. <https://doi.org/10.3402/tellusb.v55i3.16368>
- Zhuang, Q., McGuire, A. D., O'Neill, K. P., Harden, J. W., Romanovsky, V. E., & Yarie, J. (2002). Modeling soil thermal and carbon dynamics of a fire chrono sequence in interior Alaska. *Journal of Geophysical Research: Atmospheres*, 107(D1), FFR-3. <https://doi.org/10.1029/2001JD001244>
- Zhuang, Q., Romanovsky, V. E., & McGuire, A. D. (2001). Incorporation of a permafrost model into a large-scale ecosystem model: Evaluation of temporal and spatial scaling issues in simulating soil thermal dynamics. *Journal of Geophysical Research: Atmospheres*, 106(D24), 33649–33670. <https://doi.org/10.1029/2001jd900151>

References From the Supporting Information

- Fu, Y., Liu, C., Lin, F., Hu, X., Zheng, X., Zhang, W., & Cao, G. (2018). Quantification of year-round methane and nitrous oxide fluxes in a typical alpine shrub meadow on the Qinghai-Tibetan plateau. *Agriculture, Ecosystems & Environment*, 255, 27–36. <https://doi.org/10.1016/j.agee.2017.12.003>
- Goodrich, L. E. (1978). Efficient numerical technique for one-dimensional thermal problems with phase change. *International Journal of Heat and Mass Transfer*, 21(5), 615–621. [https://doi.org/10.1016/0017-9310\(78\)90058-3](https://doi.org/10.1016/0017-9310(78)90058-3)
- Huo, L., Chen, Z., Zou, Y., Lu, X., Guo, J., & Tang, X. (2013). Effect of zoige alpine wetland degradation on the density and fractions of soil organic carbon. *Ecological Engineering*, 51, 287–295. <https://doi.org/10.1016/j.ecoleng.2012.12.020>
- McGuire, A. D., Melillo, J. M., Kicklighter, D. W., Pan, Y., Xiao, X., Helfrich, J., et al. (1997). Equilibrium responses of global net primary production and carbon storage to doubled atmospheric carbon dioxide: Sensitivity to changes in vegetation nitrogen concentration. *Global Biogeochemical Cycles*, 11(2), 173–189. <https://doi.org/10.1029/97GB00059>
- Nieberding, F., Wille, C., Fratini, G., Asmussen, M. O., Wang, Y., Ma, Y., & Sachs, T. (2020). A long-term (2005–2019) eddy covariance data set of CO₂ and H₂O fluxes from the Tibetan alpine steppe. *Earth System Science Data*, 12(4), 2705–2724. <https://doi.org/10.5194/essd-12-2705-2020>
- Pan, Y., Melillo, J. M., McGuire, A. D., Kicklighter, D. W., Pitelka, L. F., Hibbard, K., et al. (1998). Modeled responses of terrestrial ecosystems to elevated atmospheric CO₂: A comparison of simulations by the biogeochemistry models of the vegetation/ecosystem modeling and analysis project (VEMAP). *Oecologia*, 114(3), 389–404. <https://doi.org/10.1007/s004420050462>
- Shang, W., Wu, X. D., Zhao, L., Yue, G. Y., Zhao, Y. H., Qiao, Y. P., & Li, Y. Q. (2016). Seasonal variations in labile soil organic matter fractions in permafrost soils with different vegetation types in the central Qinghai-Tibet plateau. *Catena*, 137, 670–678. <https://doi.org/10.1016/j.catena.2015.07.012>
- Tao, Z., Shen, C., Gao, Q., Sun, Y., Yi, W., & Li, Y. (2007). Soil organic carbon storage and soil CO₂ flux in the alpine meadow ecosystem. *Science in China - Series D: Earth Sciences*, 50(7), 1103–1114. <https://doi.org/10.1007/s11430-007-0055-3>
- Tian, H., Melillo, J. M., Kicklighter, D. W., McGuire, A. D., & Helfrich, J. (1999). The sensitivity of terrestrial carbon storage to historical climate variability and atmospheric CO₂ in the United States. *Tellus B: Chemical and Physical Meteorology*, 51(2), 414–452. <https://doi.org/10.3402/tellusb.v51i2.16318>